



BodyNet: Volumetric Inference of 3D Human Body Shapes



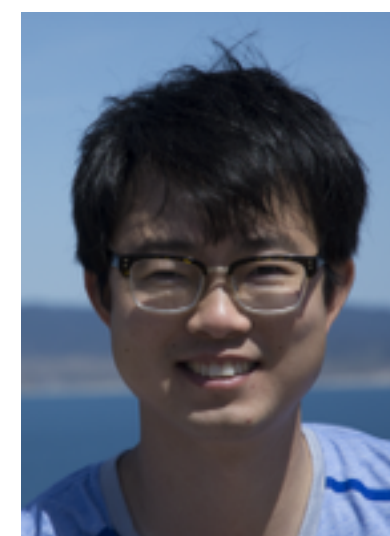
Gul Varol¹



Duygu Ceylan²



Bryan Russell²



Jimei Yang²



Ersin Yumer²



Ivan Laptev¹



Cordelia Schmid¹

¹Inria, ²Adobe Research

Goal

RGB input

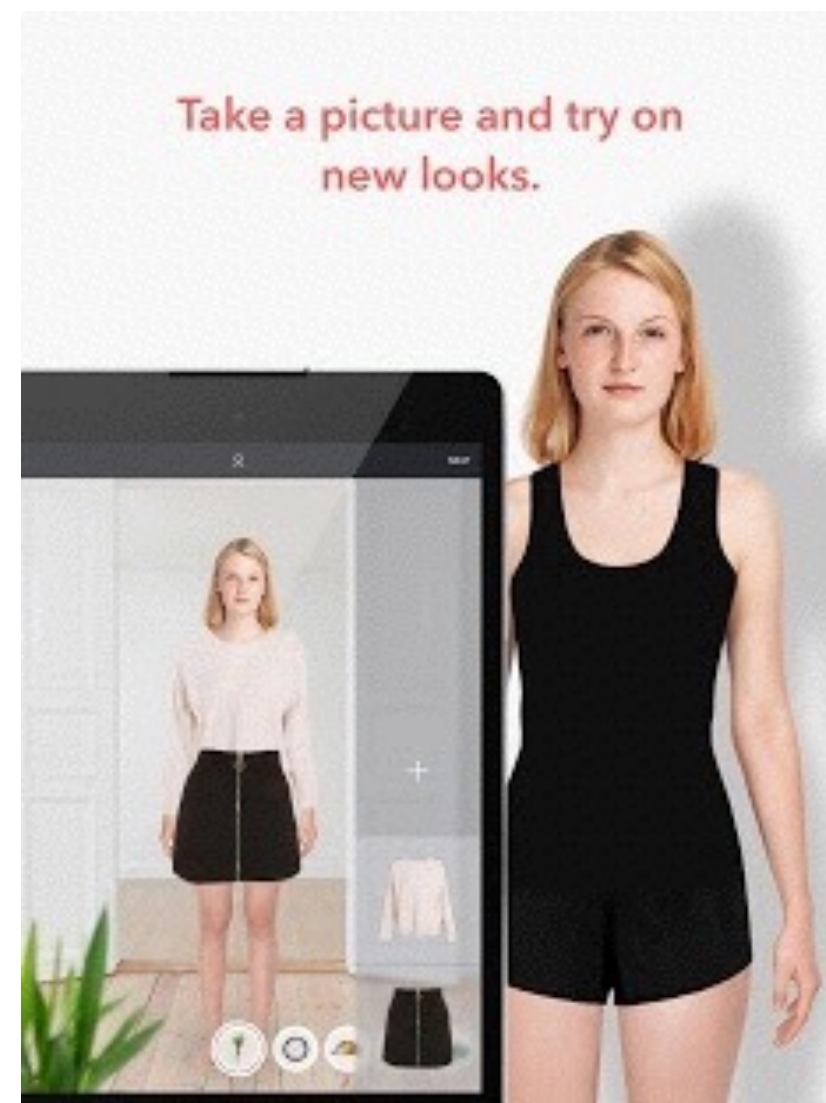


Output 3D shape prediction



Why?

Virtual try-on



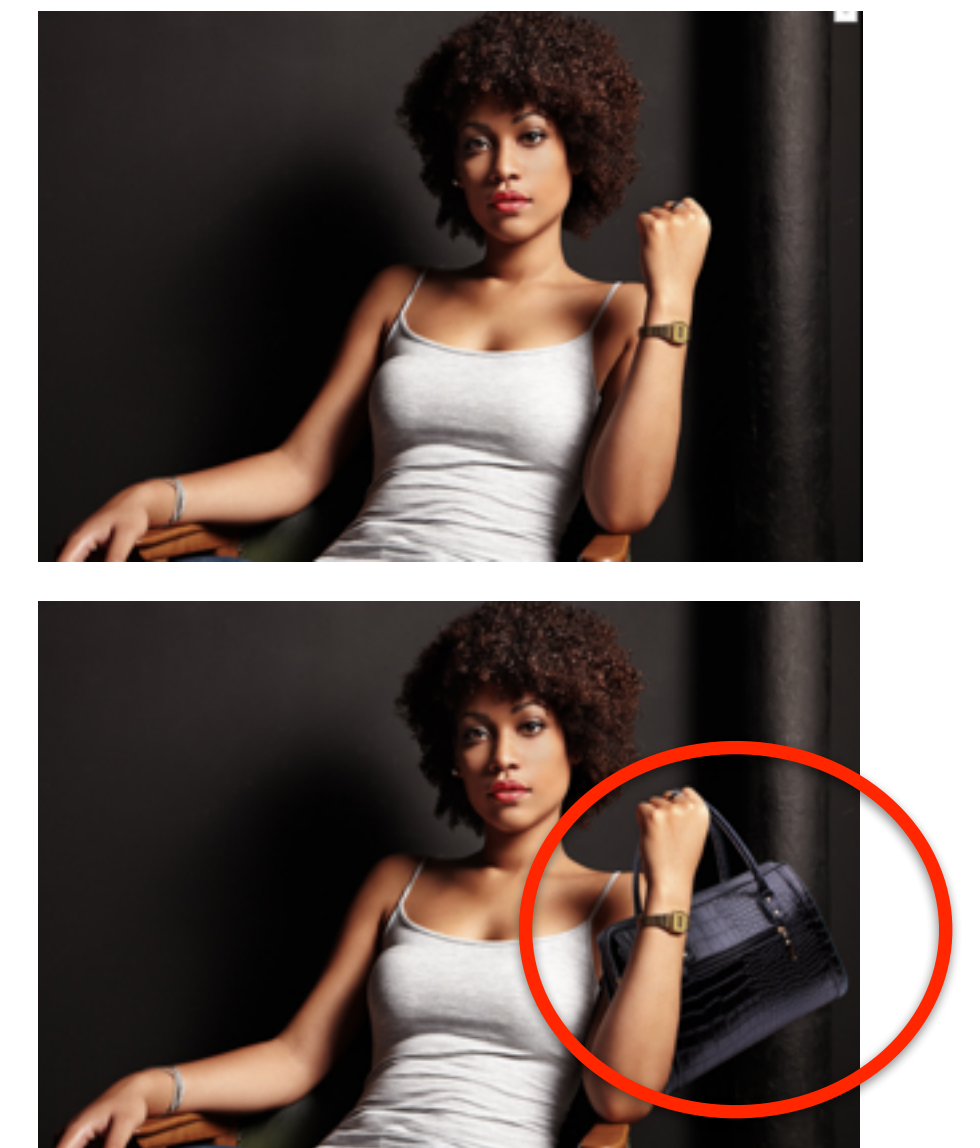
Pictofit

Creation of digital avatars



ToFit

Human-aware editing



Adobe

Why?

Healthcare



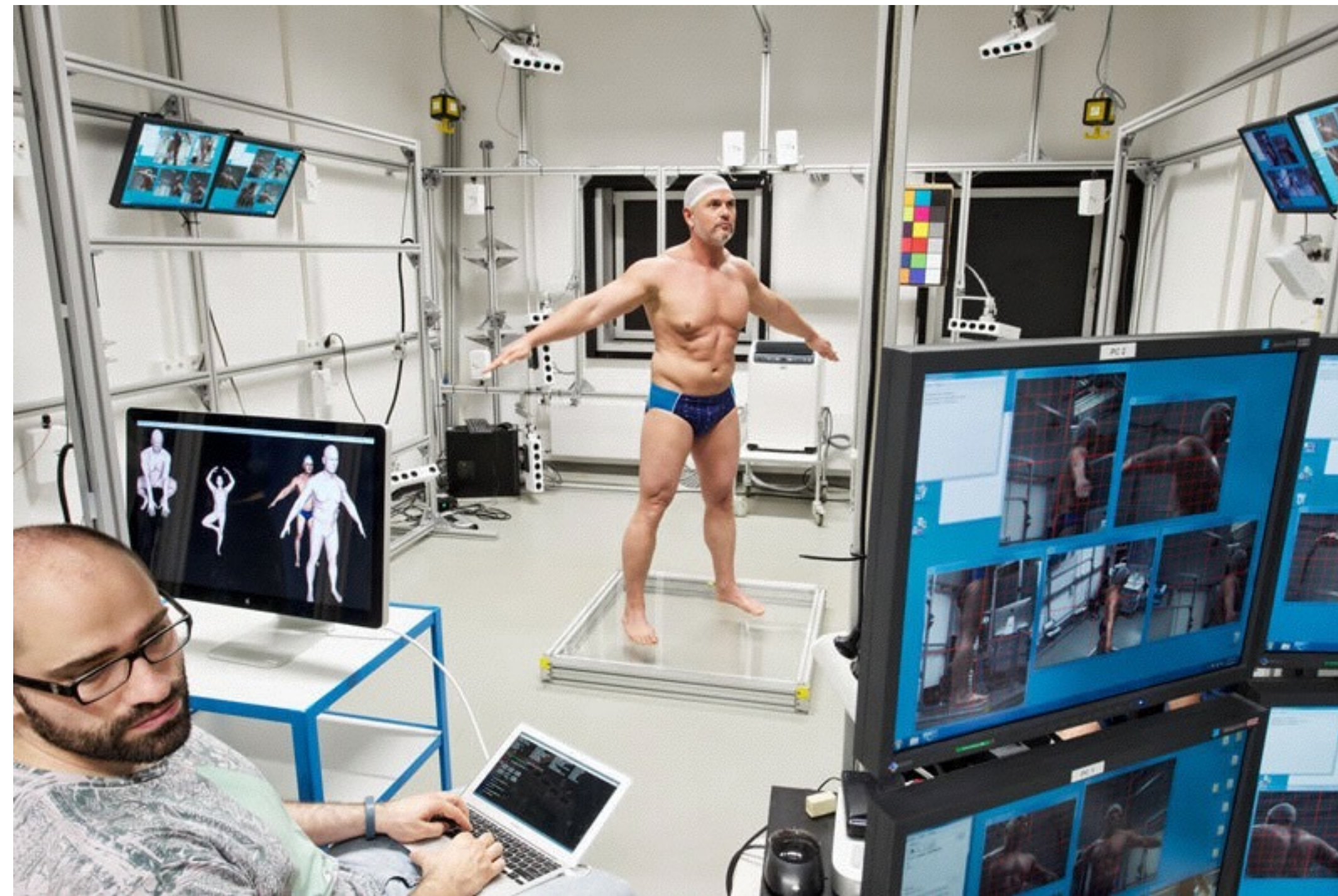
mPort

Action recognition / Surveillance



Challenges - Difficult without Scanner

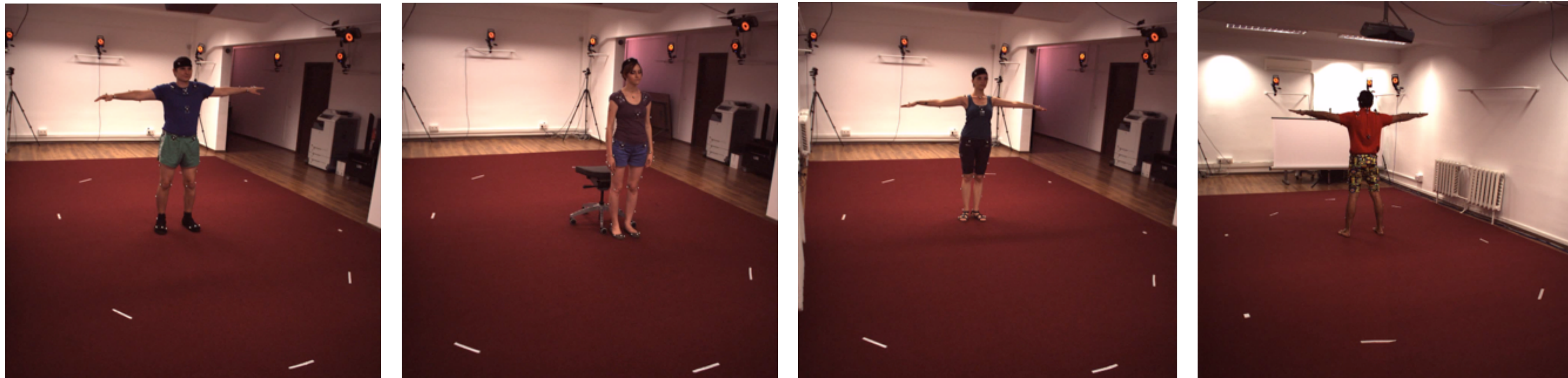
- Existing methods recovering 3D body shape rely mostly on complex scanners



Max Planck Institute, Germany

Challenges - Lack of Data

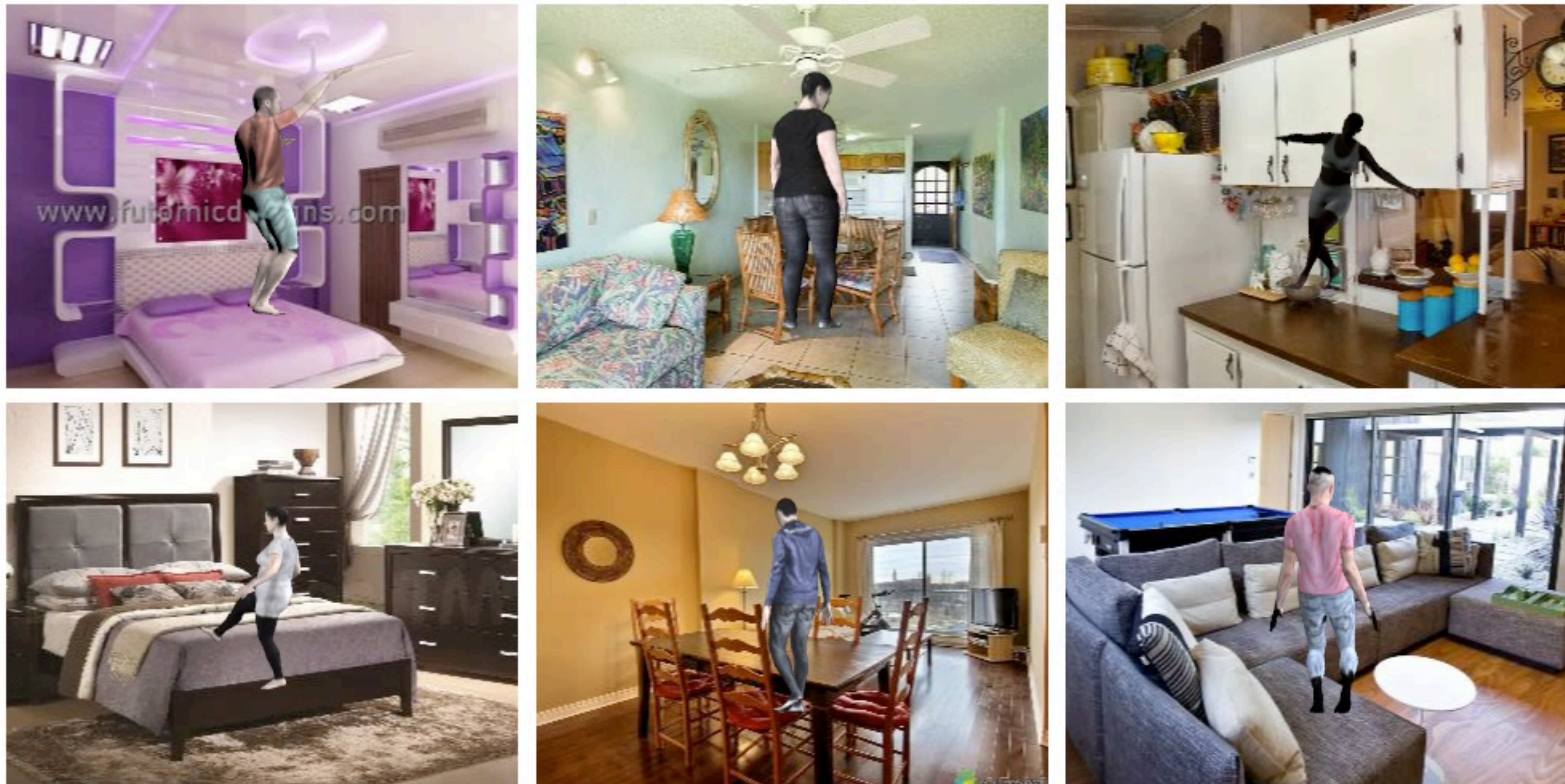
- Full 3D shape data is available either in **constrained settings...**



Ionescu et al. Human3.6M: Large Scale Datasets and Predictive Methods for 3D Human Sensing in Natural Environments, TPAMI 2014

Challenges - Lack of Data

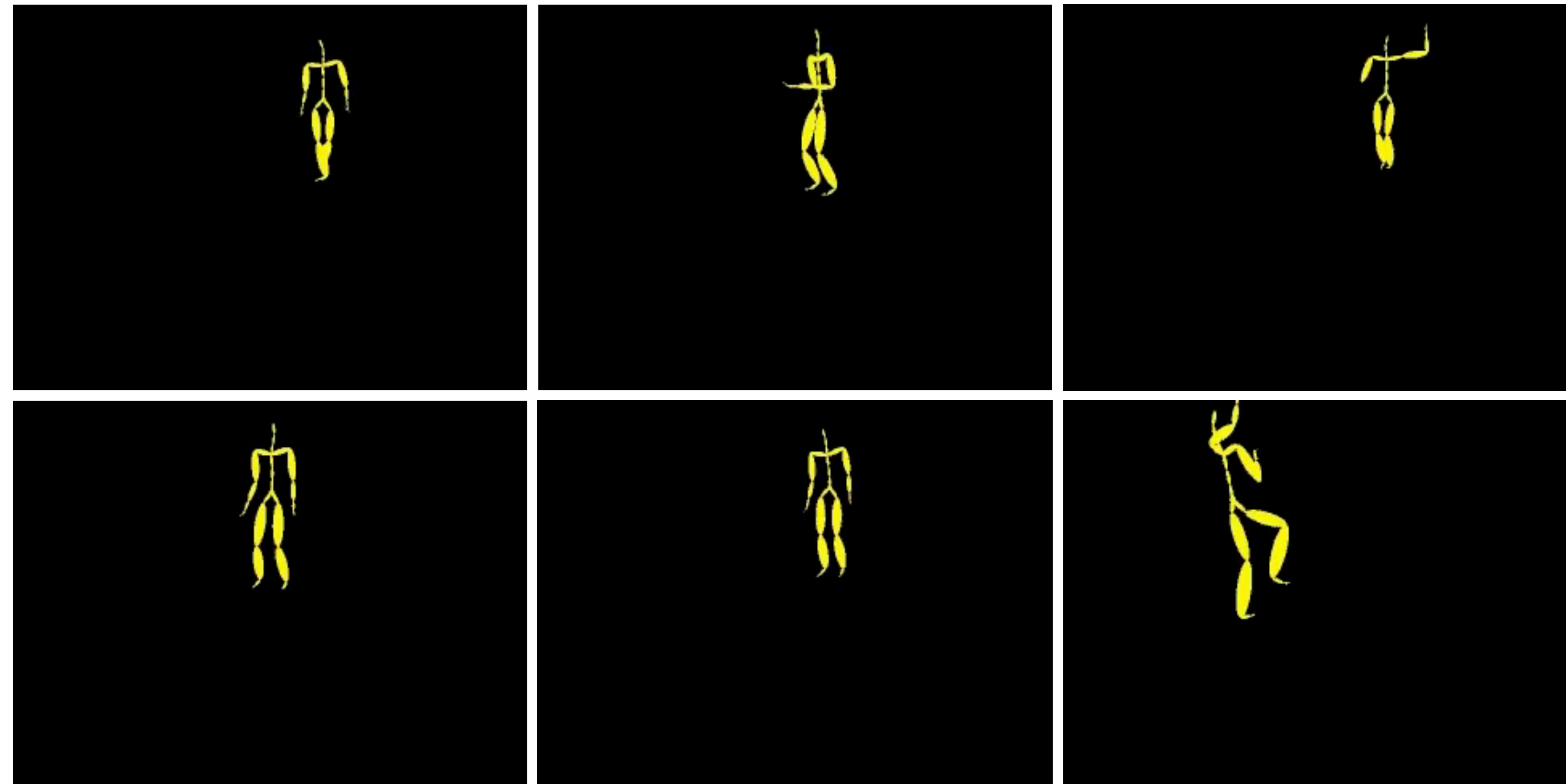
- Full 3D shape data is available either in constrained settings **or synthetic**



Varol et al. Learning from Synthetic Humans, CVPR 2017

Challenges - Lack of Data

- Most methods focus on predicting a skeleton

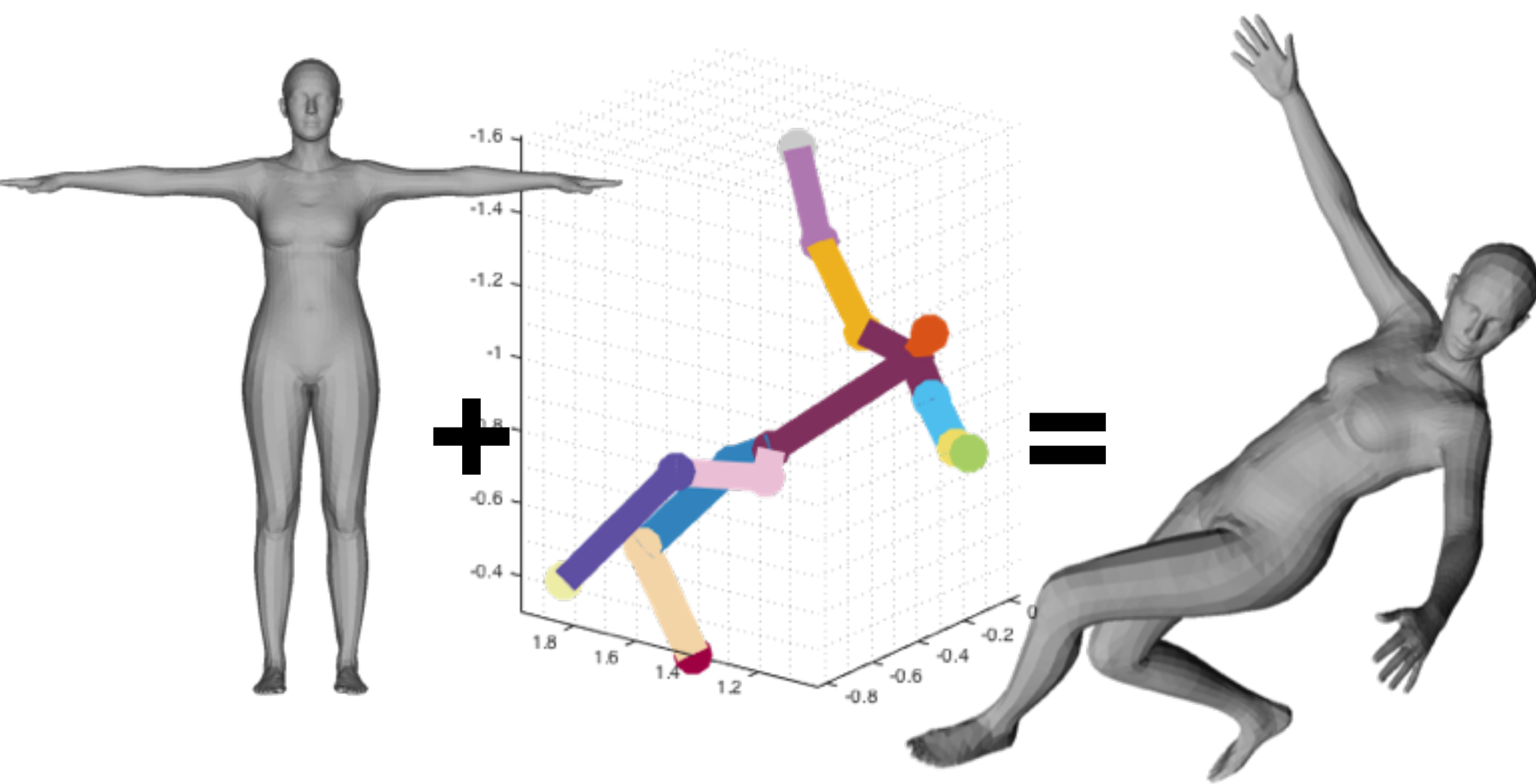


CMU MoCap Database

Challenges - Representation

$$10 + 72 = 82$$

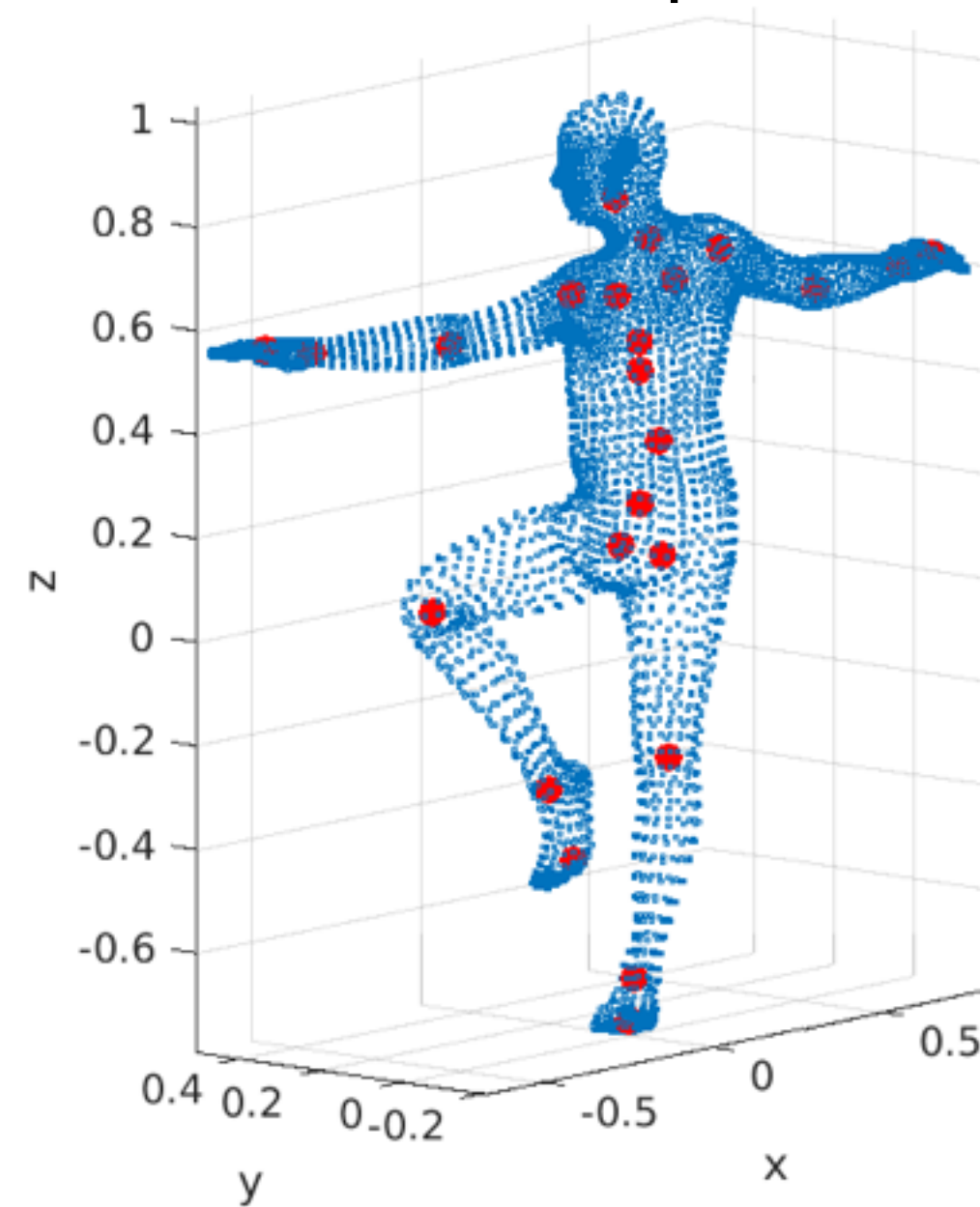
Parametric representation



Loper et al. [1]

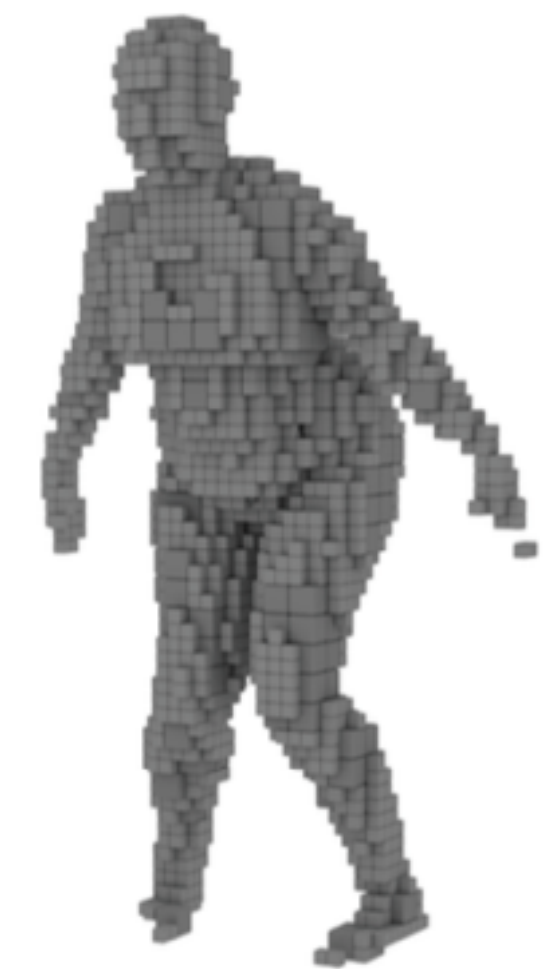
$$6890 \times 3 = 20670$$

Point cloud representation



$$64^3 = 262144$$

Voxel representation



Tatarchenko et al. [2]

[1] Loper et al. SMPL: A Skinned Multi-Person Linear Model, SIGGRAPH Asia 2015

[2] Tatarchenko et al. Octree Generating Networks: Efficient Convolutional Architectures for High-resolution 3D Outputs, ICCV 2017

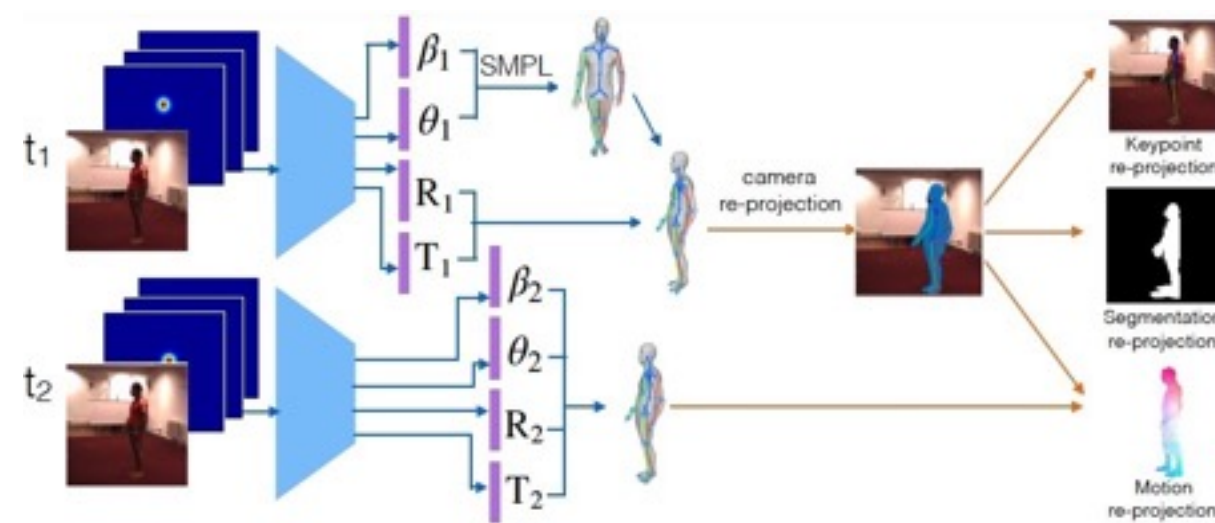
3D Human Body Shape Representation in the literature



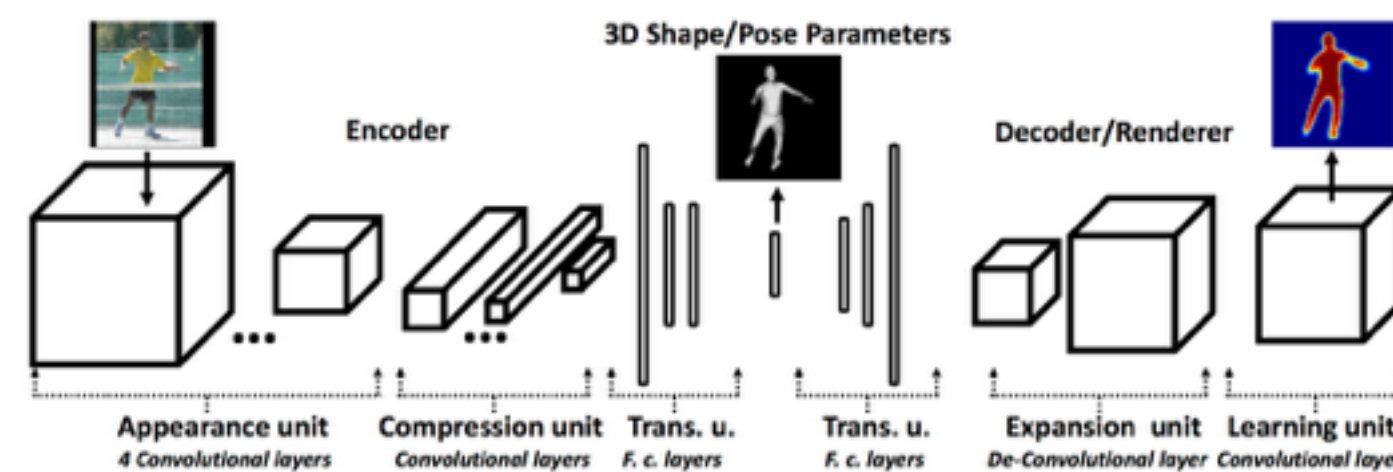
SMPLify - Bogo et al. ECCV 2016



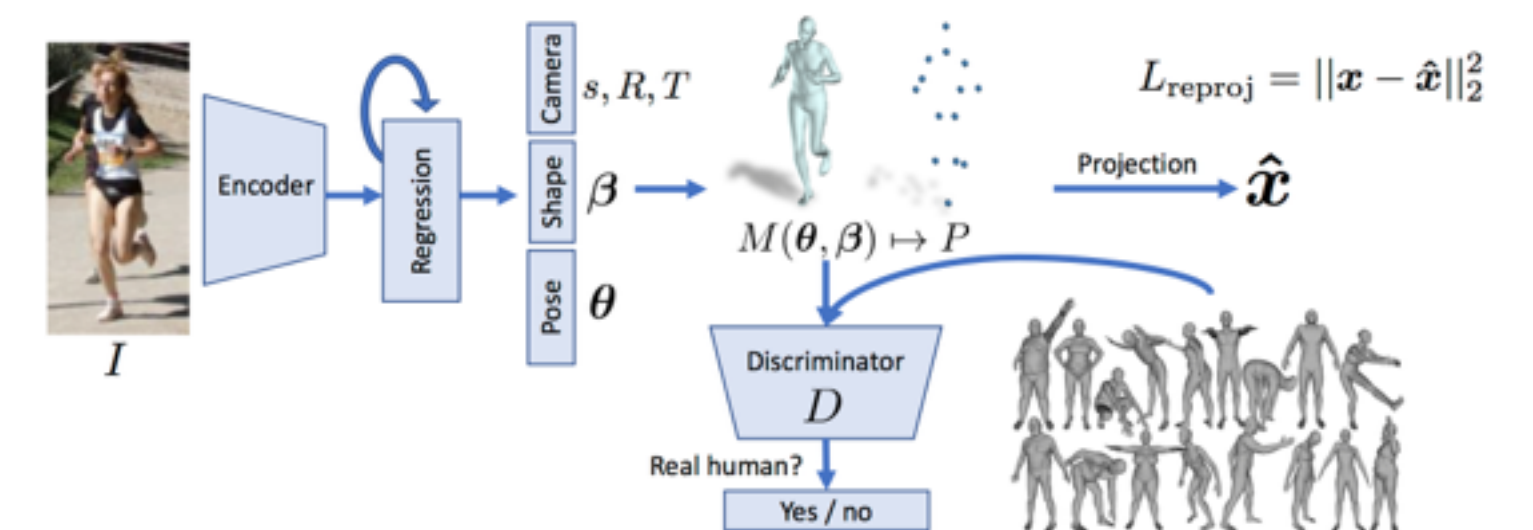
Unite the People - Lassner et al. CVPR 2017



Self-supervised learning - Tung et al. NIPS 2017

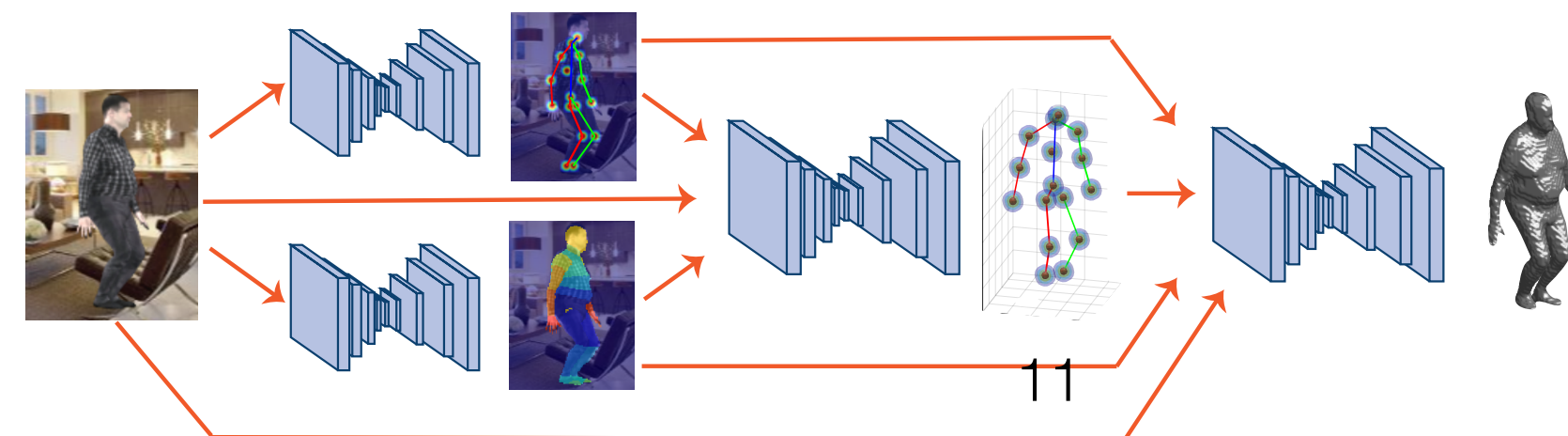
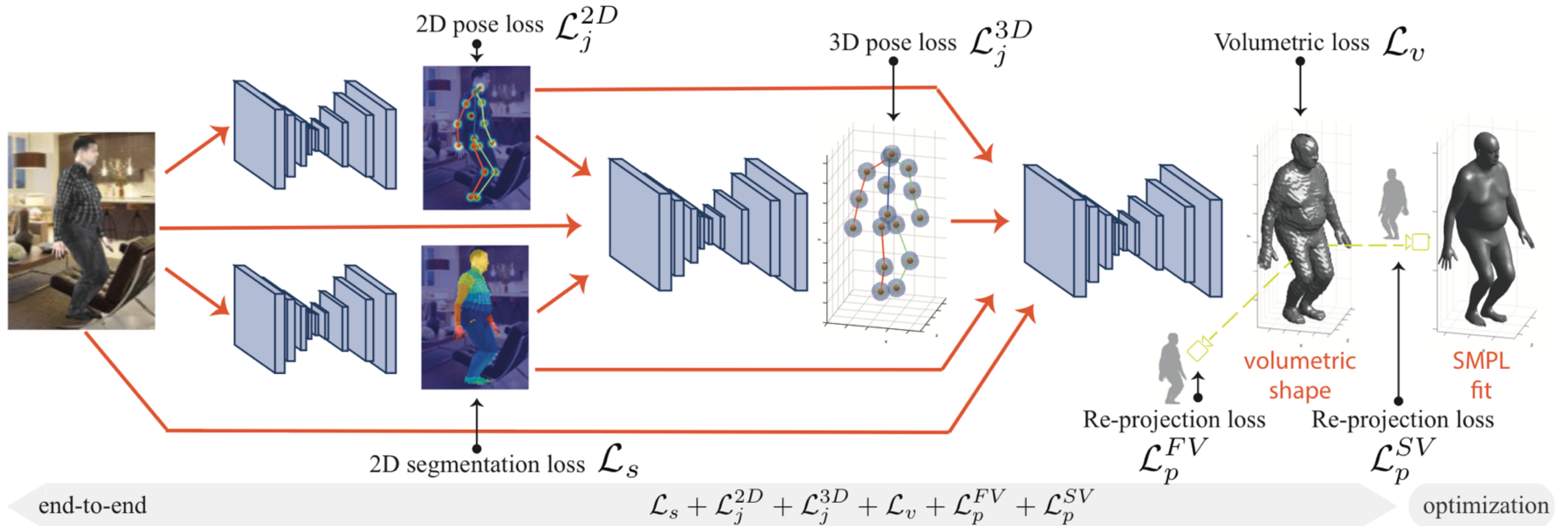


Indirect learning - Tan et al. BMVC 2017



HMR - Kanazawa et al. CVPR 2018

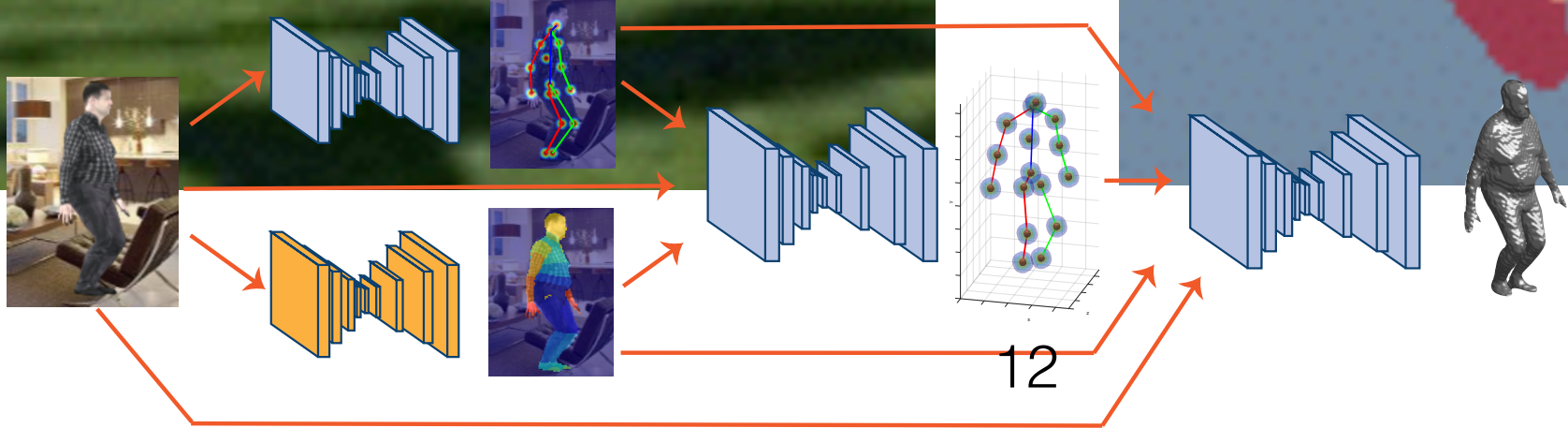
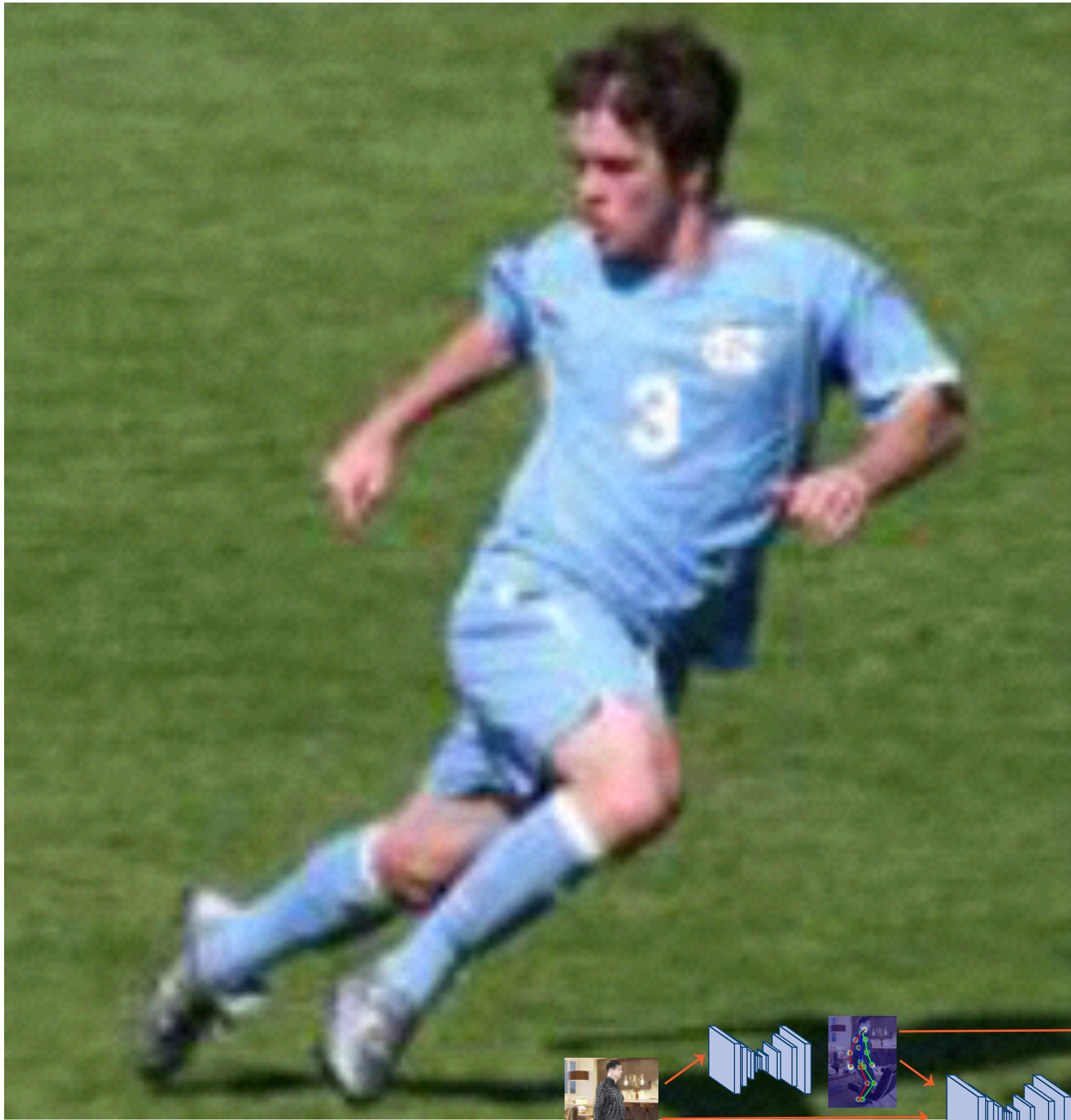
Proposed method: BodyNet



Subnetwork 1:

RGB input

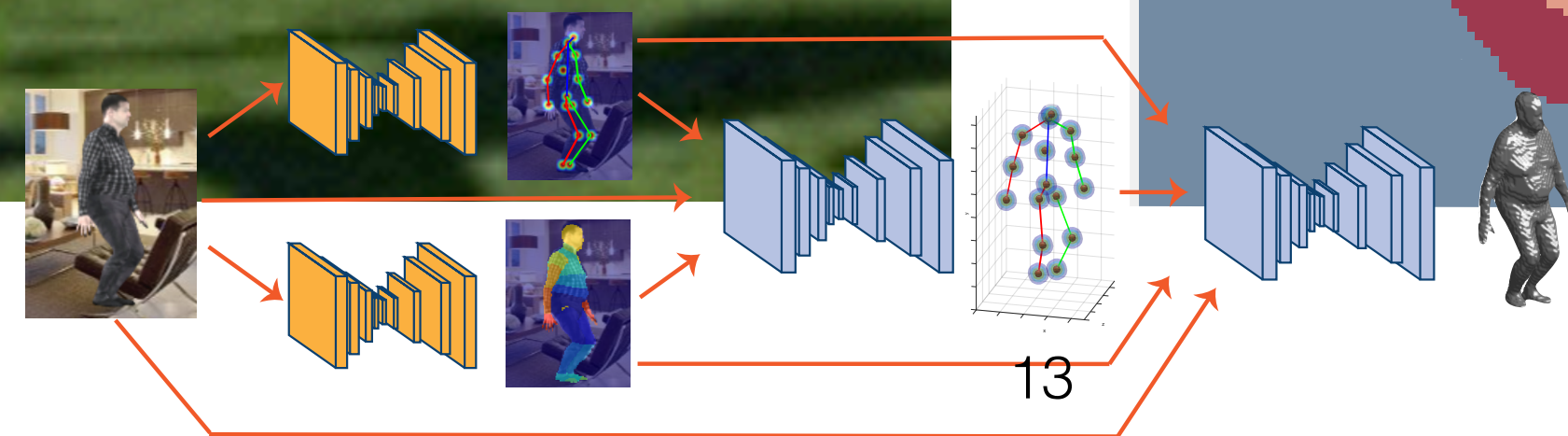
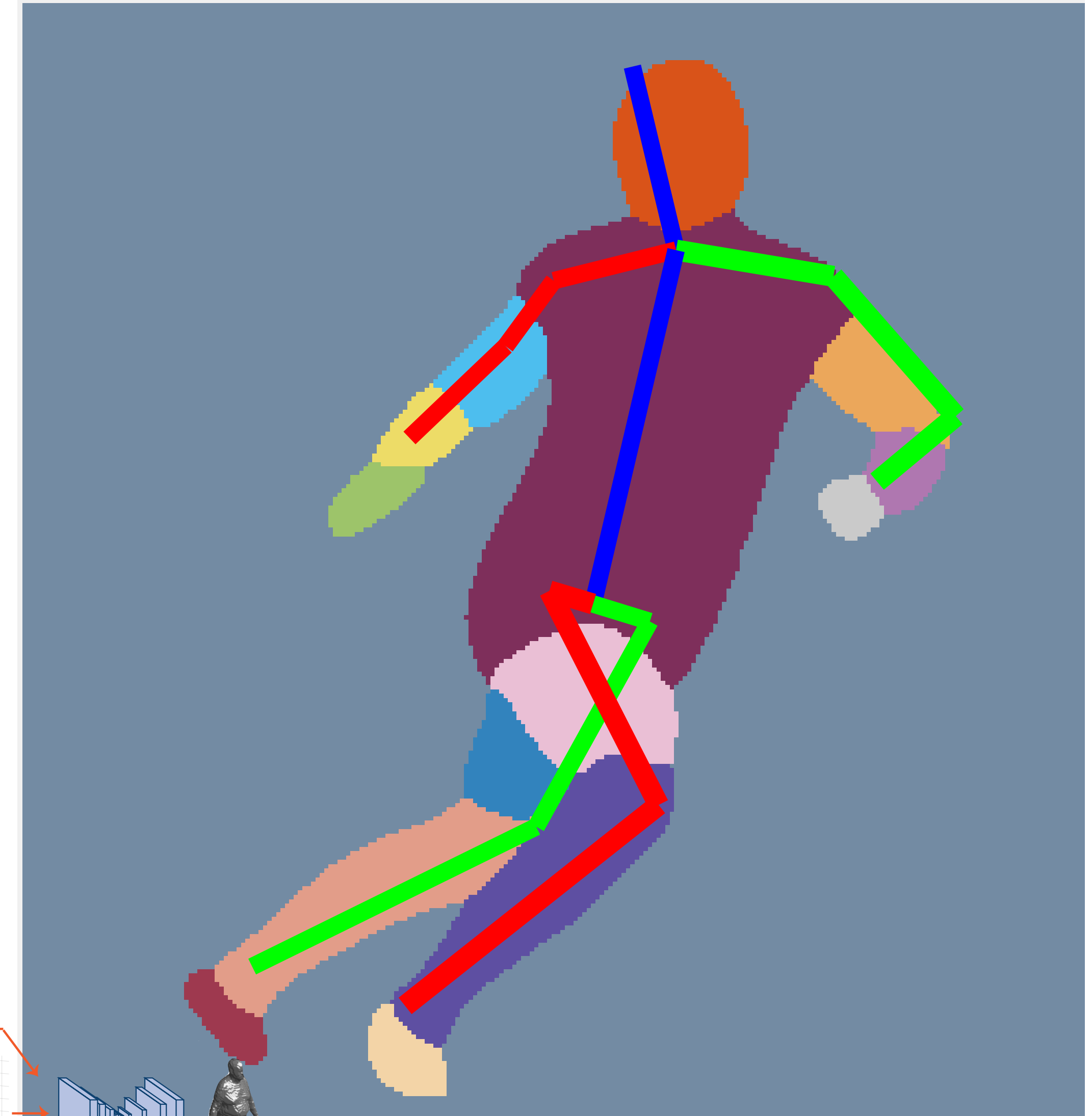
2D segmentation



Subnetwork 1&2:

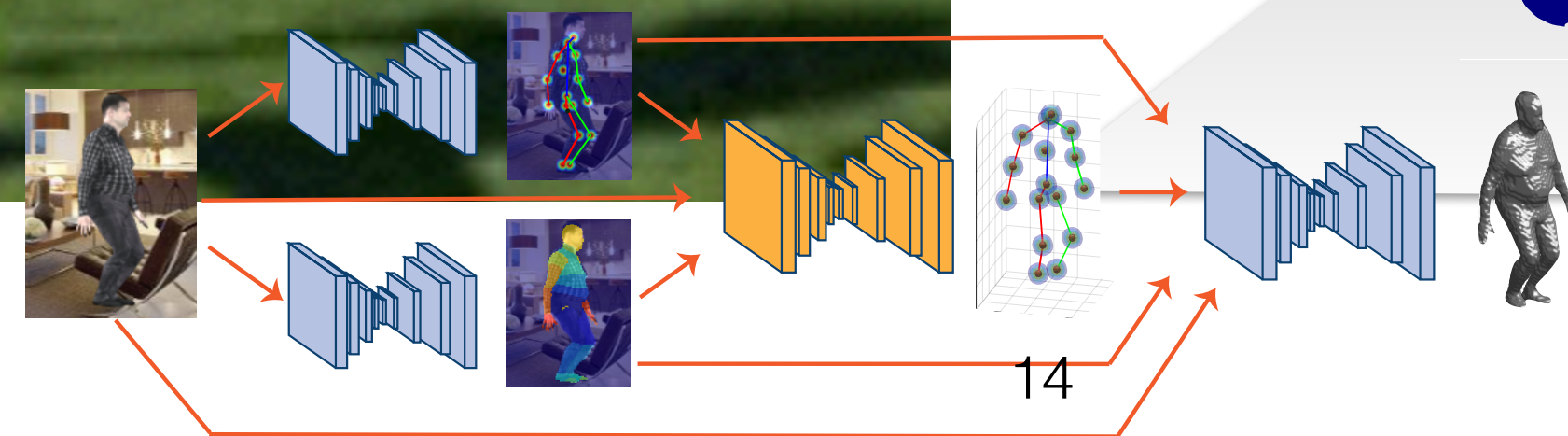
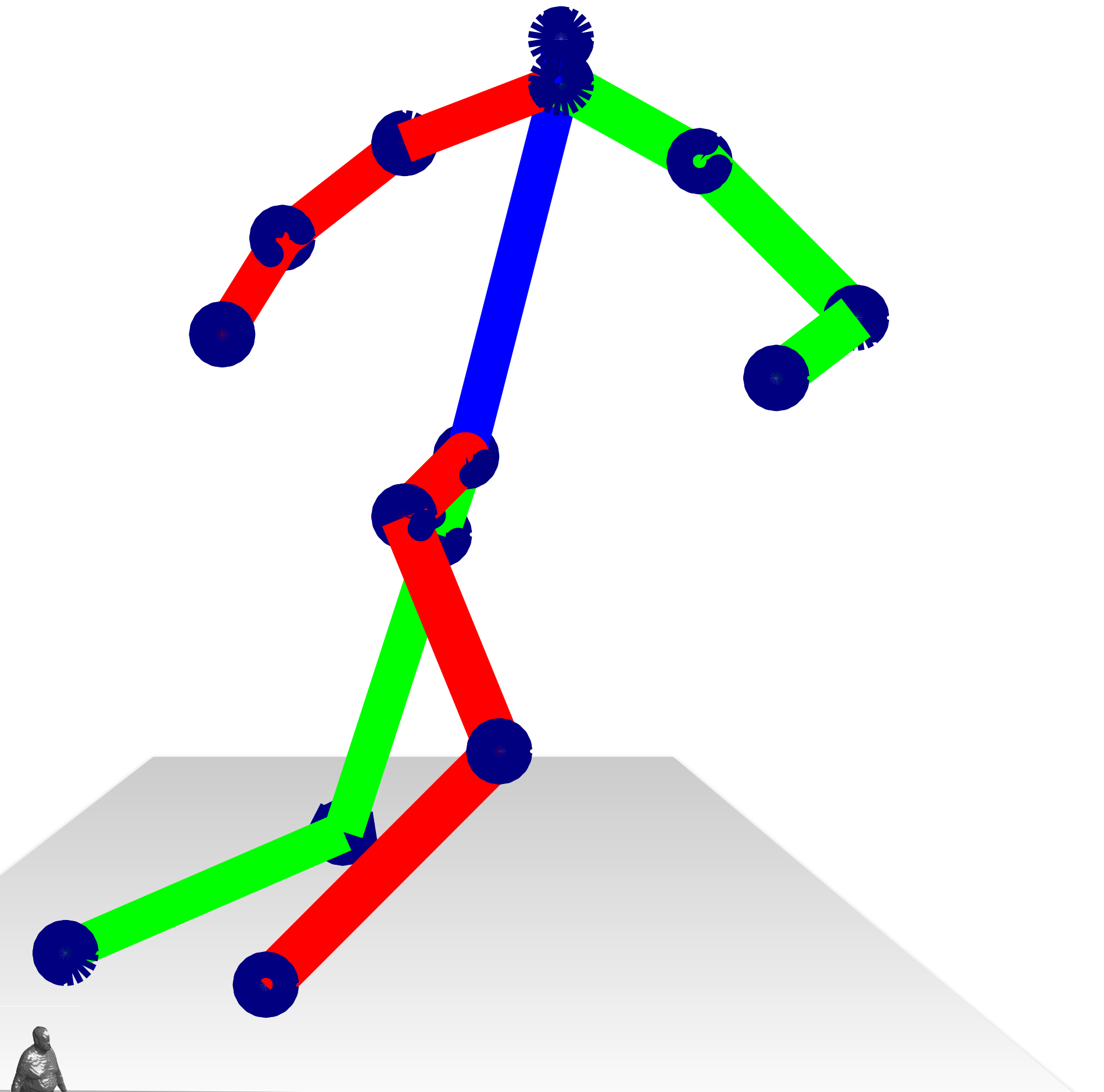
RGB input

2D segmentation & 2D pose predictions



RGB input

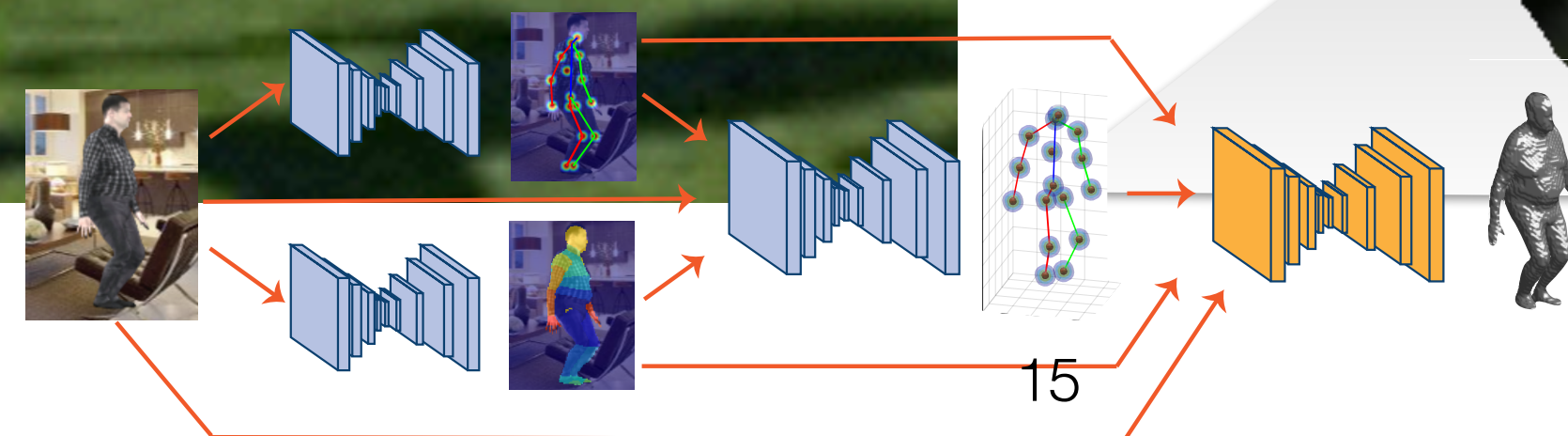
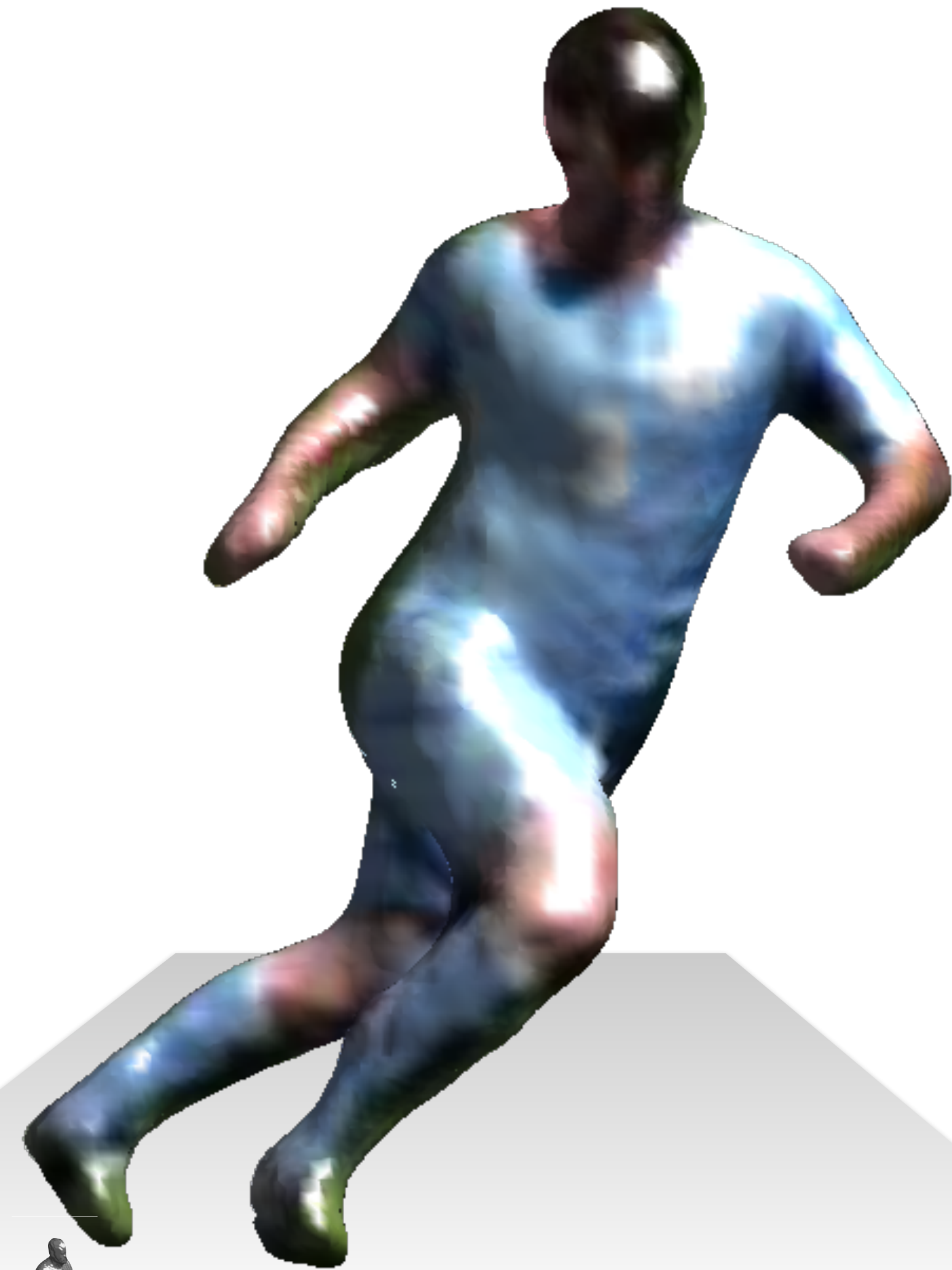
Subnetwork 3:
3D pose prediction



RGB input

Subnetwork 4:

Volumetric shape prediction



RGB input



(Optional) Fitting:
SMPL



RGB input

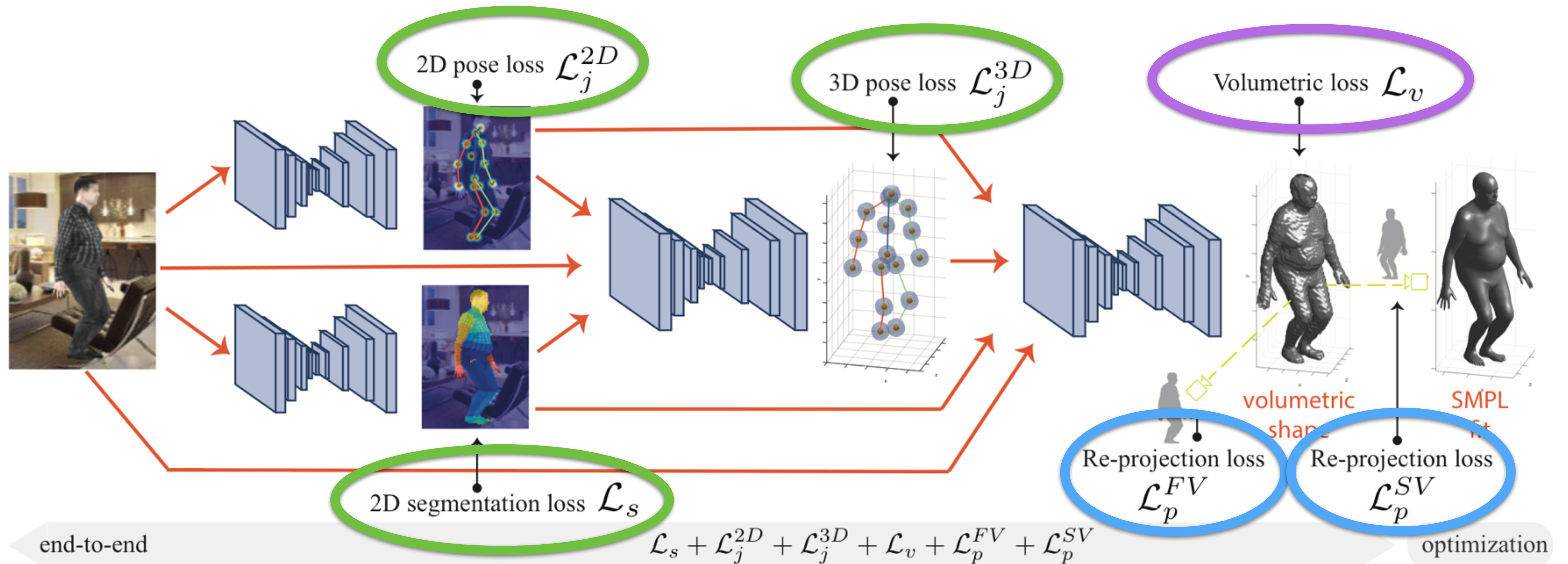


Output 3D body parts prediction



BodyNet is an end-to-end trainable network that benefits from:

- a volumetric 3D loss,
- a multi-view re-projection loss,
- intermediate supervision of 2D pose, 2D body part segmentation, and 3D pose.



- **volumetric 3D loss**

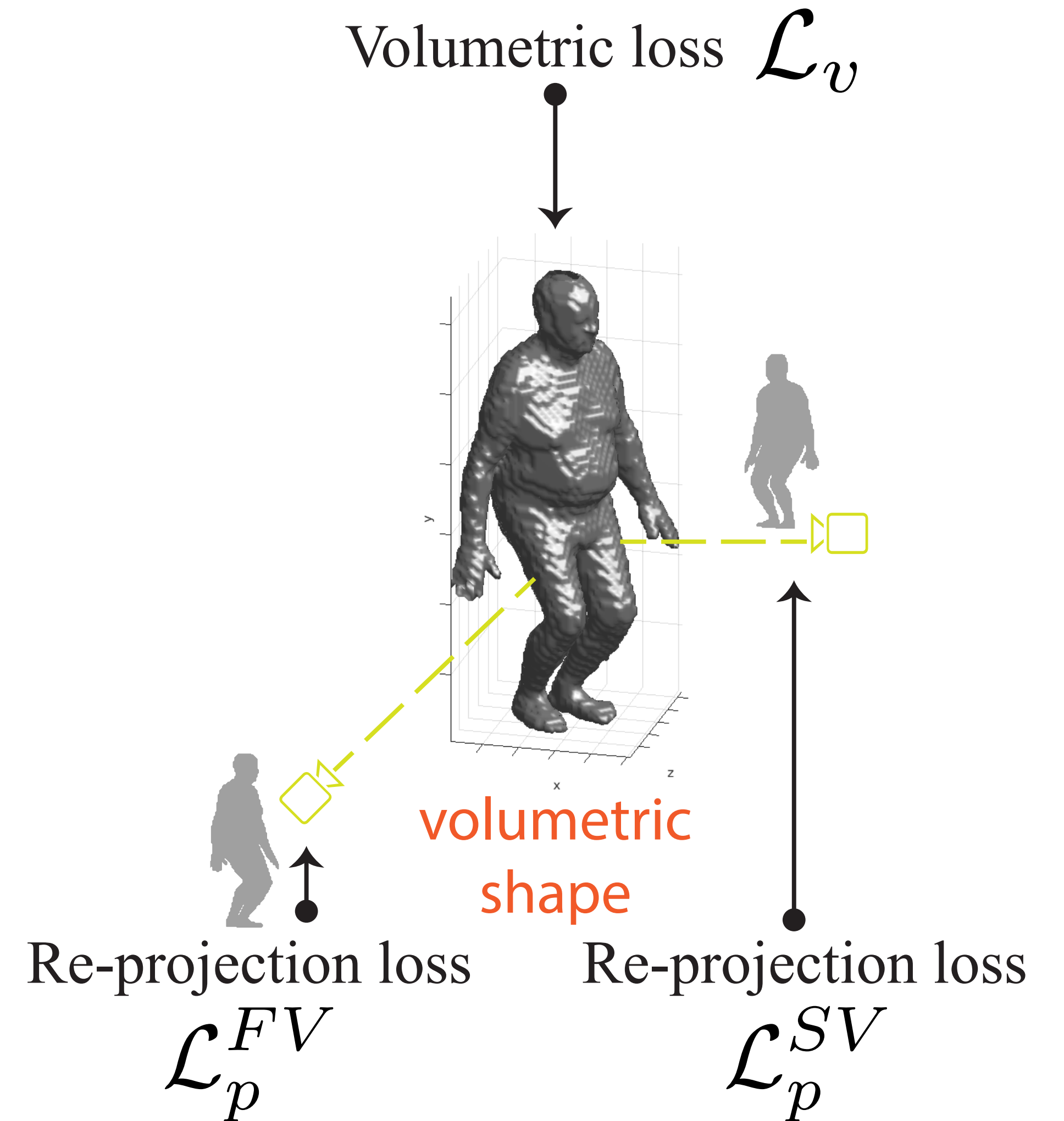
$$\mathcal{L}_v = \sum_{x=1}^W \sum_{y=1}^H \sum_{z=1}^D V_{xyz} \log \hat{V}_{xyz} + (1 - V_{xyz}) \log(1 - \hat{V}_{xyz})$$

- **multi-view re-projection loss**

$$\hat{S}^{FV}(x, y) = \max_z \hat{V}_{xyz} \quad \text{and} \quad \hat{S}^{SV}(y, z) = \max_x \hat{V}_{xyz}.$$

$$\mathcal{L}_p^{FV} = \sum_{x=1}^W \sum_{y=1}^H S(x, y) \log \hat{S}^{FV}(x, y) + (1 - S(x, y)) \log(1 - \hat{S}^{FV}(x, y)),$$

$$\mathcal{L}_p^{SV} = \sum_{y=1}^H \sum_{z=1}^D S(y, z) \log \hat{S}^{SV}(y, z) + (1 - S(y, z)) \log(1 - \hat{S}^{SV}(y, z)).$$



SMPL fitting

$$\{\theta^*, \beta^*\} = \operatorname{argmin}_{\{\theta, \beta\}} \sum_{\mathbf{p}^n \in \mathbf{V}^n} \min_{\mathbf{p}^s \in \mathbf{V}^s(\theta, \beta)} w^n \|\mathbf{p}^n - \mathbf{p}^s\|_2^2 +$$

$$\sum_{\mathbf{p}^s \in \mathbf{V}^s(\theta, \beta)} \min_{\mathbf{p}^n \in \mathbf{V}^n} w^n \|\mathbf{p}^n - \mathbf{p}^s\|_2^2 + \lambda \sum_{i=1}^J \|\mathbf{j}_i^n - \mathbf{j}_i^s(\theta, \beta)\|_2^2.$$

θ Pose parameter of SMPL

β Shape parameter of SMPL

\mathbf{p}^n Vertex coordinate predicted by the network

\mathbf{p}^s Closest vertex coordinate of fitted SMPL

\mathbf{j}_i^n 3D joint coordinate predicted by the network

\mathbf{j}_i^s 3D joint coordinate of fitted SMPL

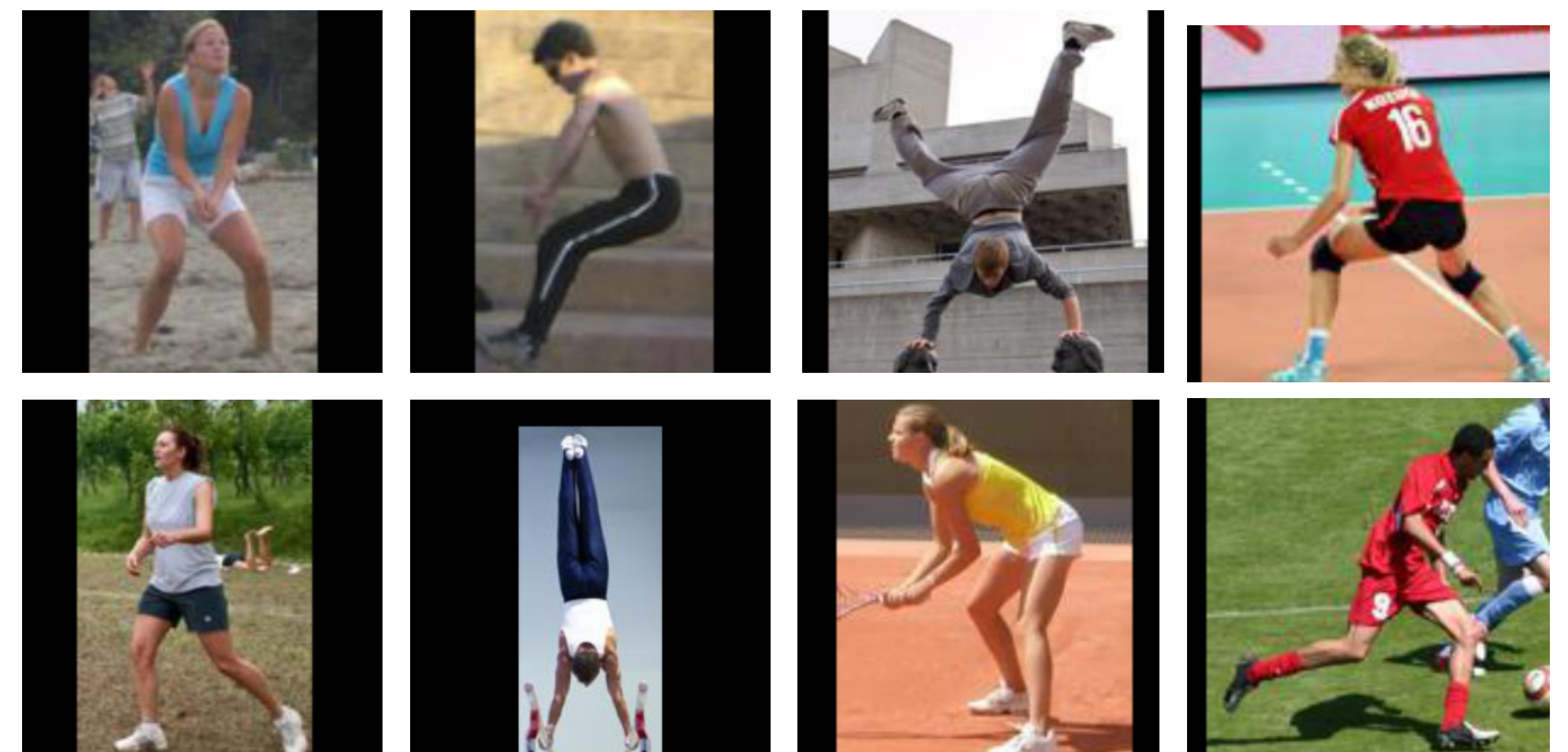


Experiments - Datasets

- **SURREAL** (Varol et al. CVPR 2017)
 - synthetically rendered images
 - perfect ground truth

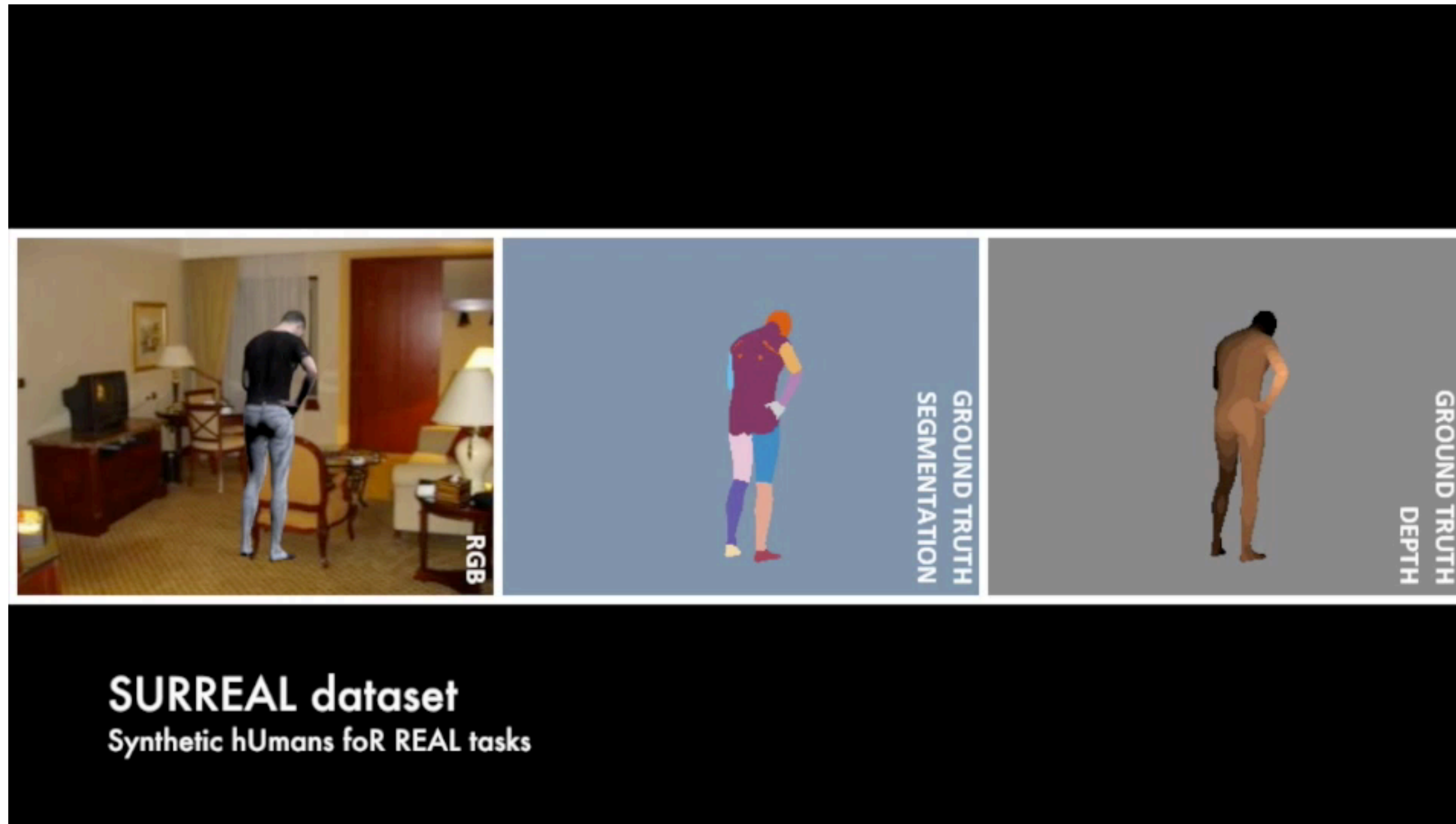


- **Unite the People** (Lassner et al. CVPR 2017)
 - real images
 - noisy 3D ground truth
 - manual 2D segmentation annotation



SURREAL Dataset

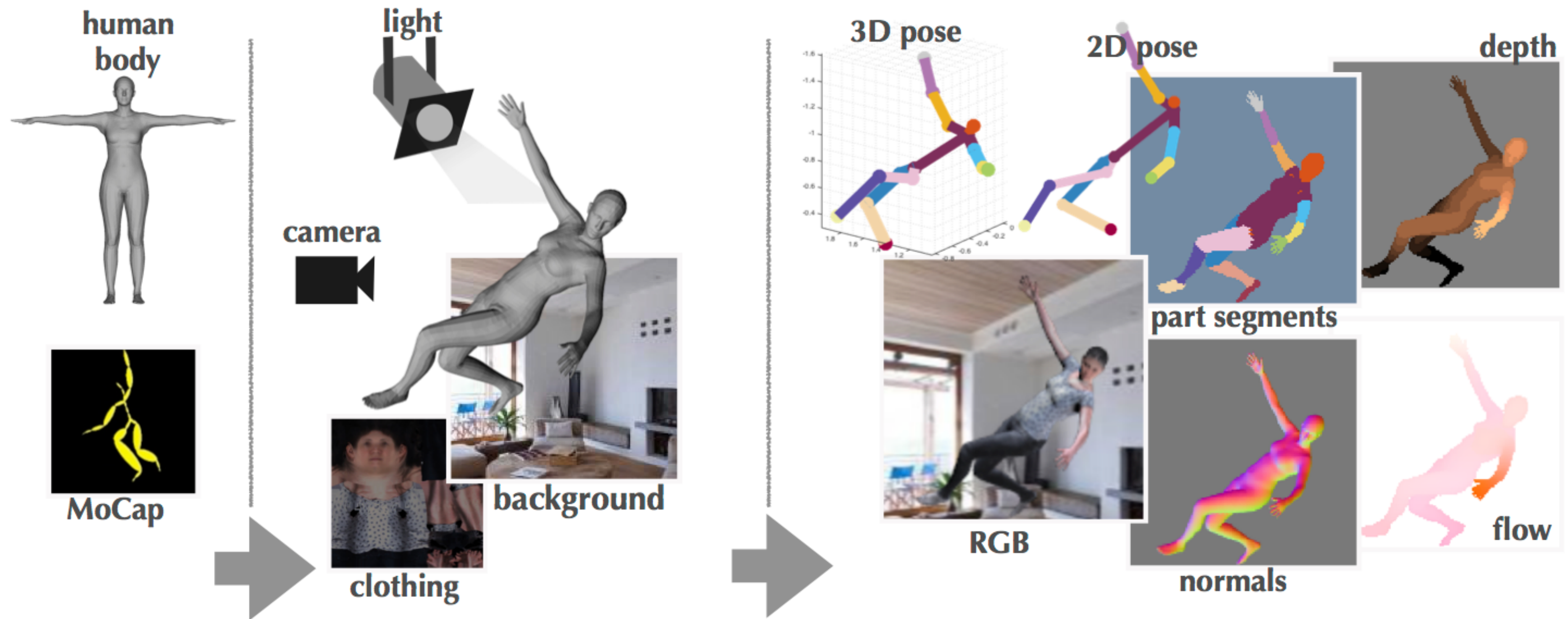
Synthetic hUmans foR REAL tasks



Varol et al. Learning from Synthetic Humans, CVPR 2017

SURREAL Dataset

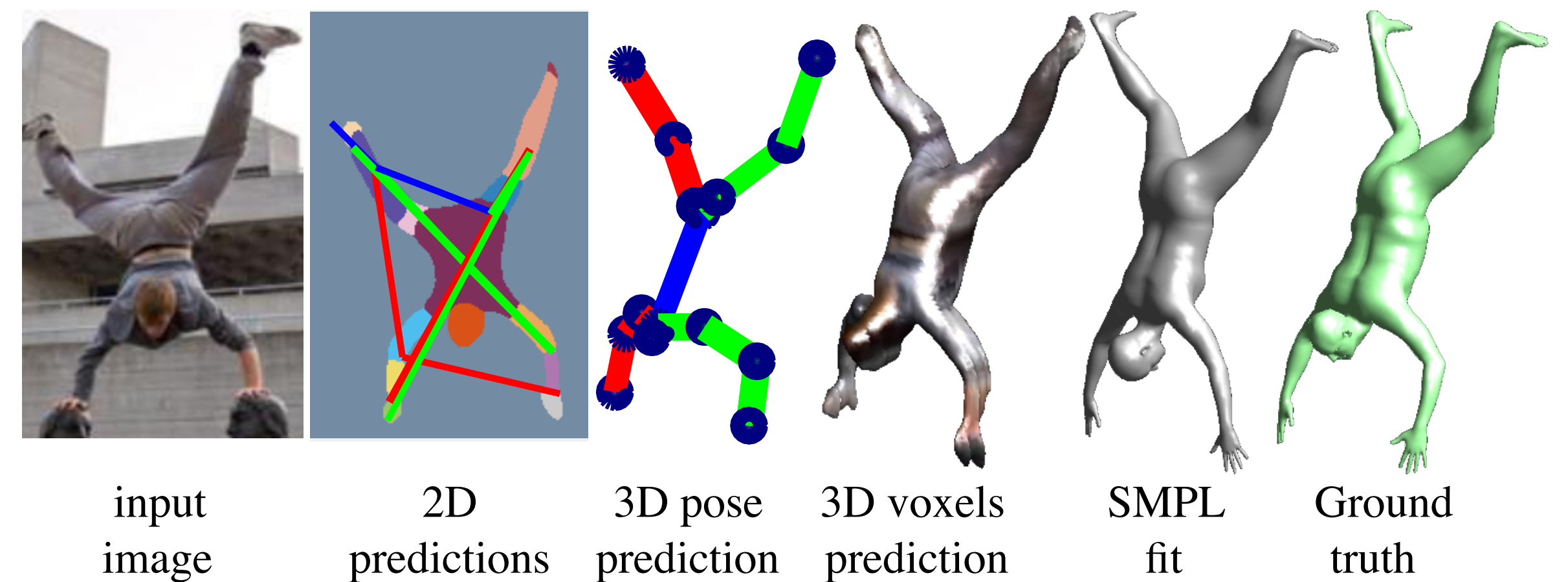
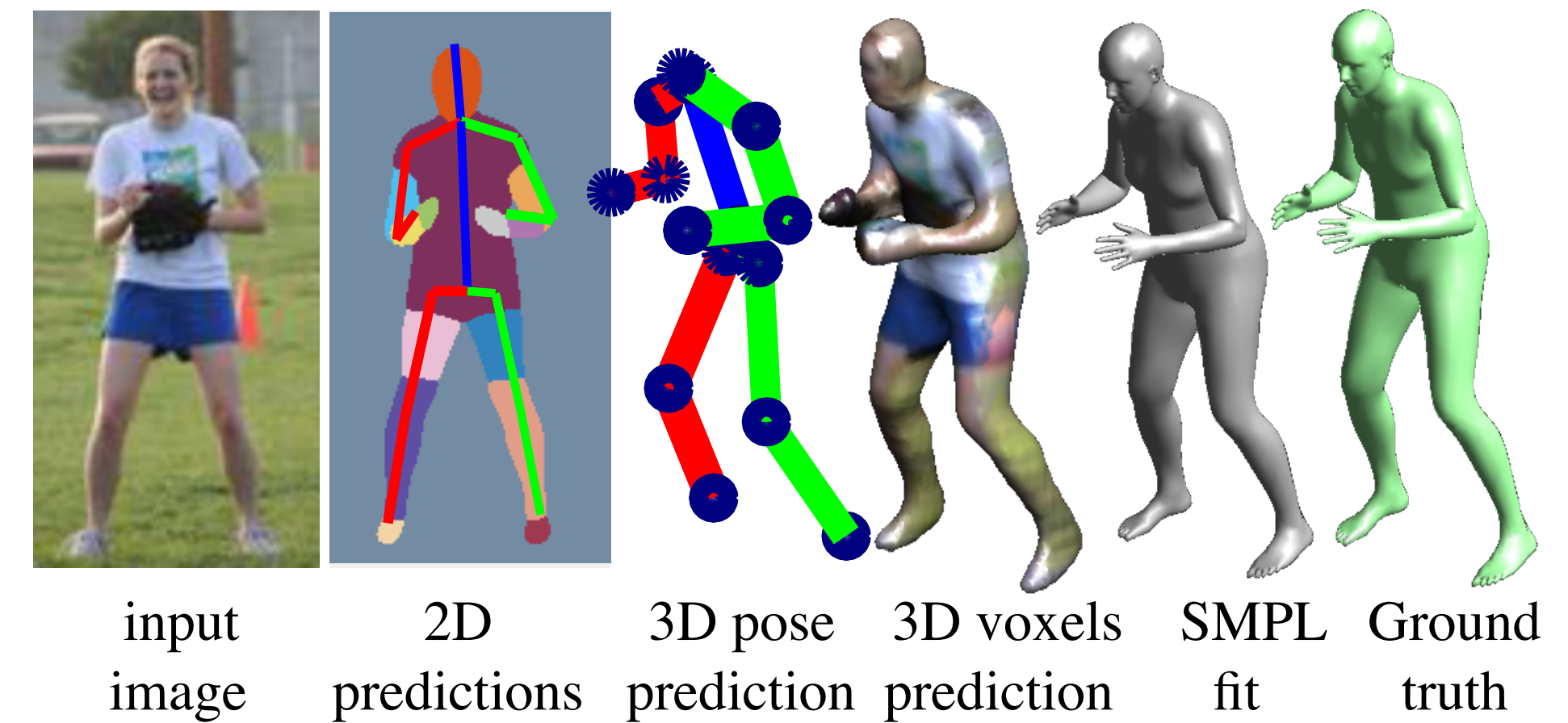
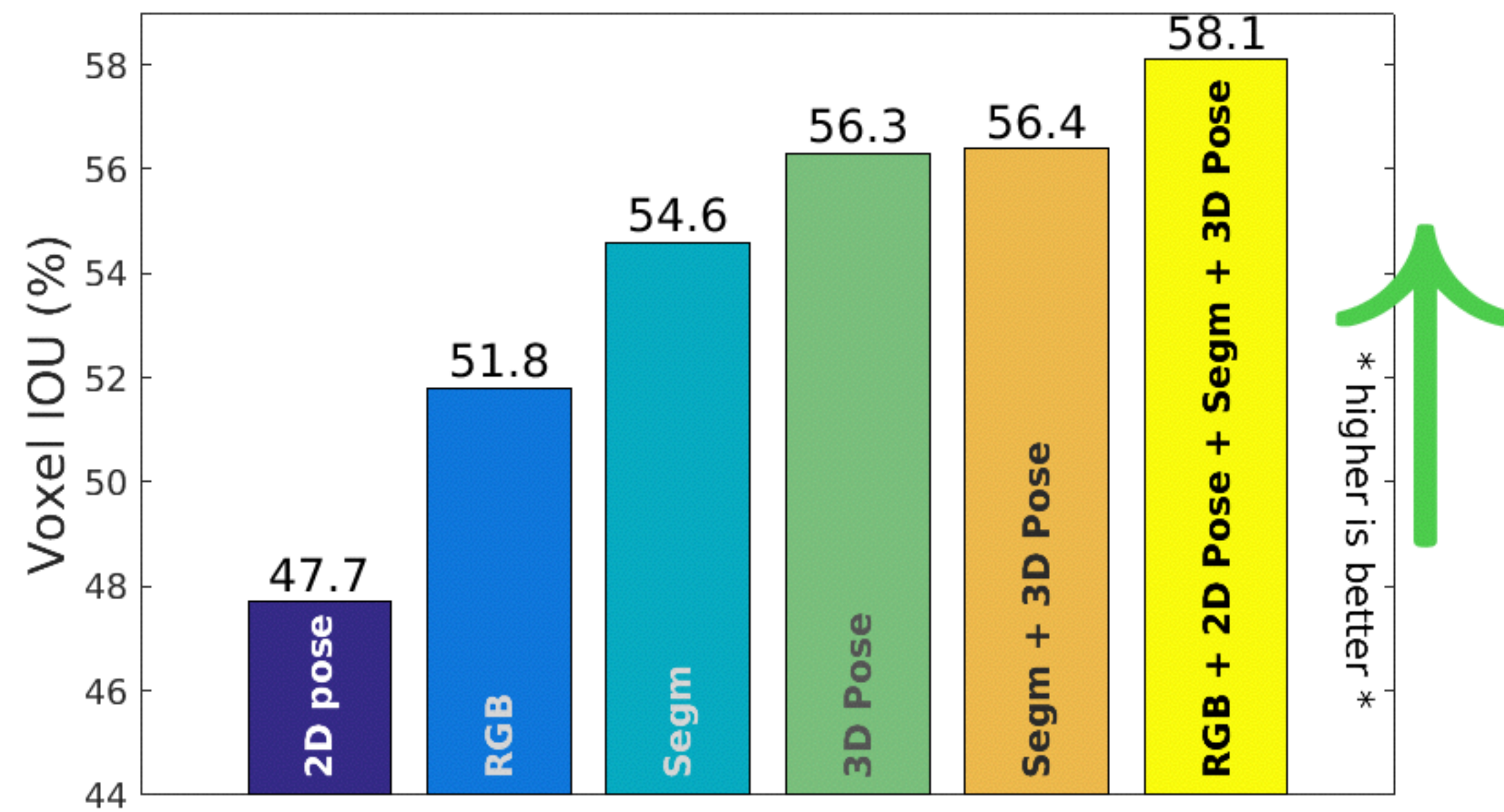
Synthetic hUmans foR REAL tasks



Varol et al. Learning from Synthetic Humans, CVPR 2017

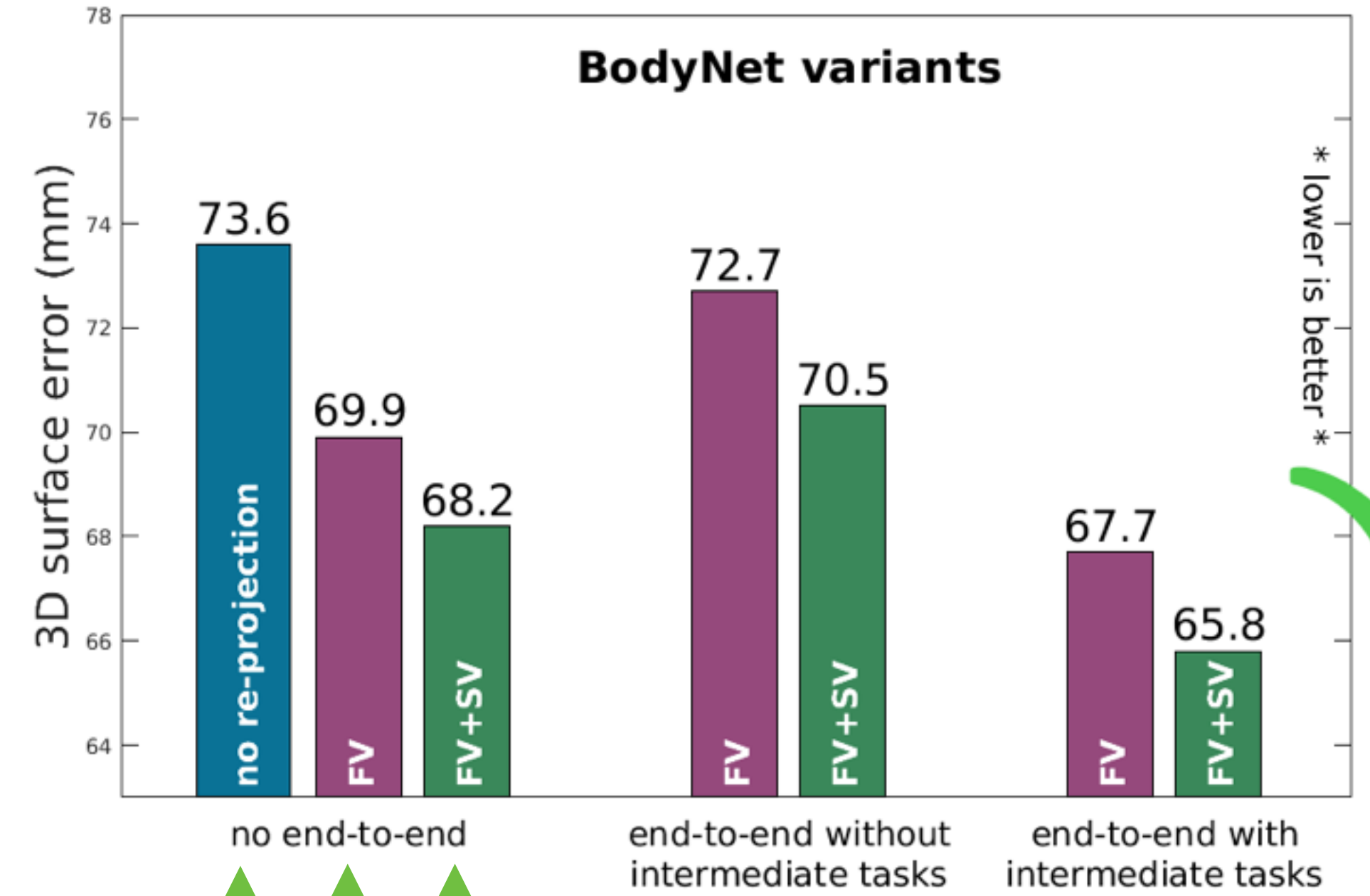
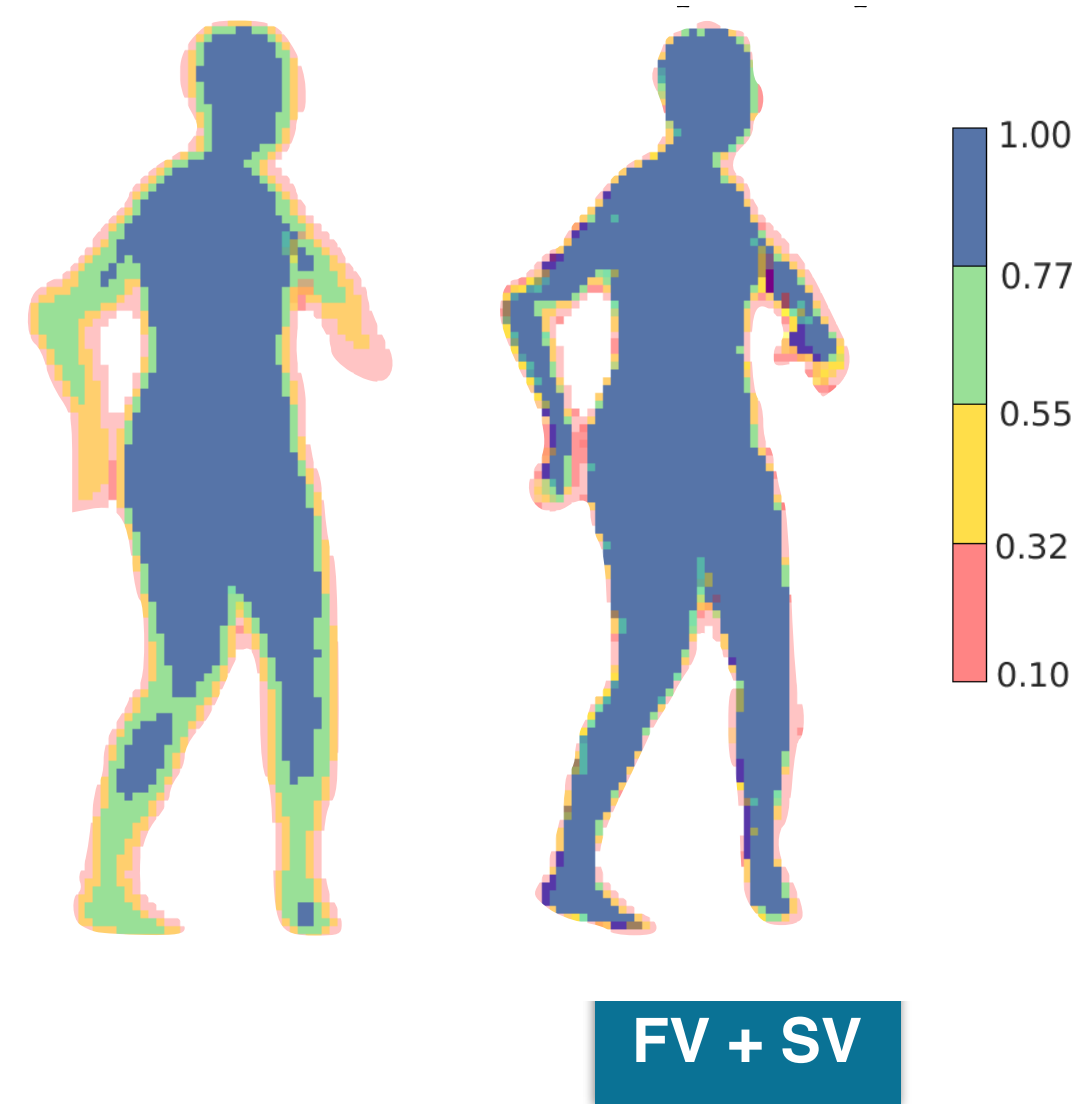
Experiments

- Effect of additional inputs



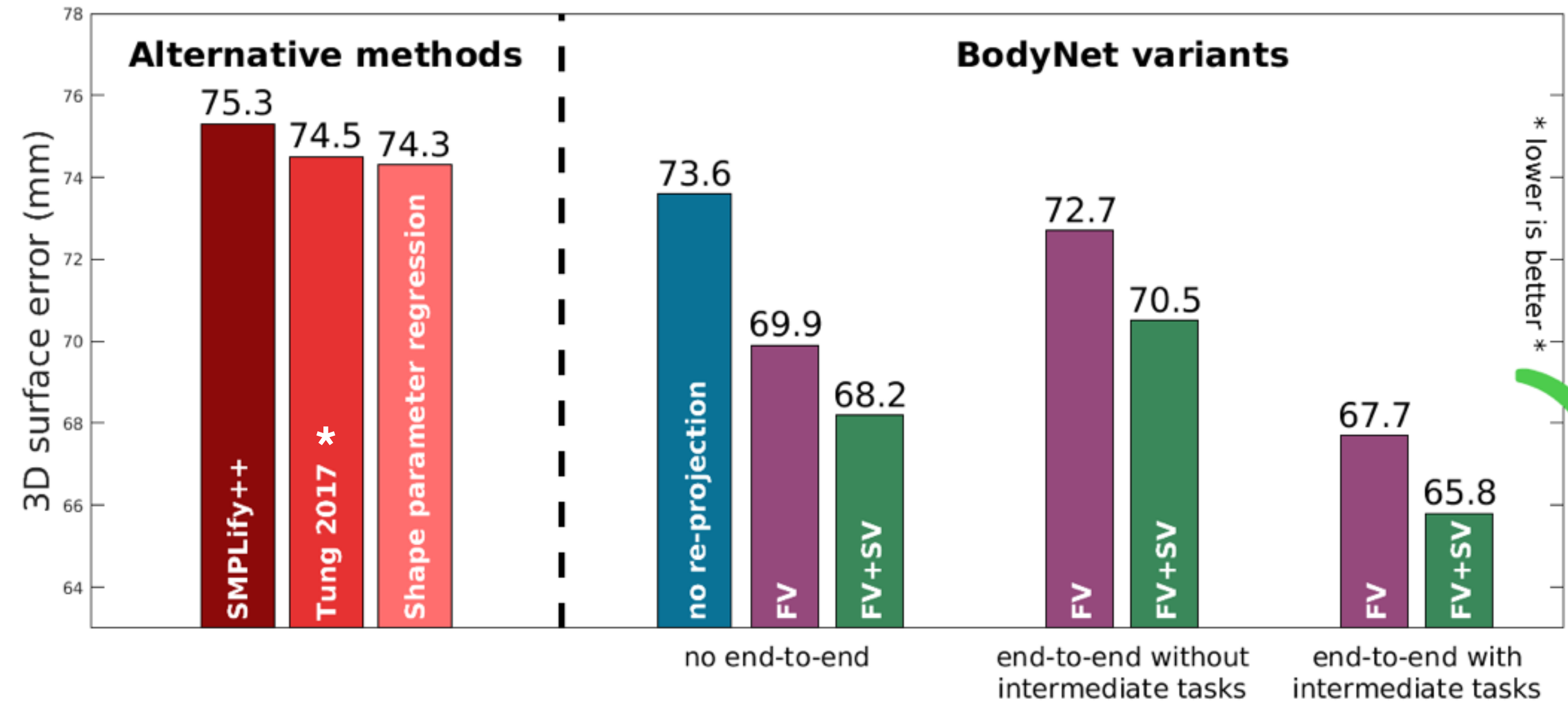
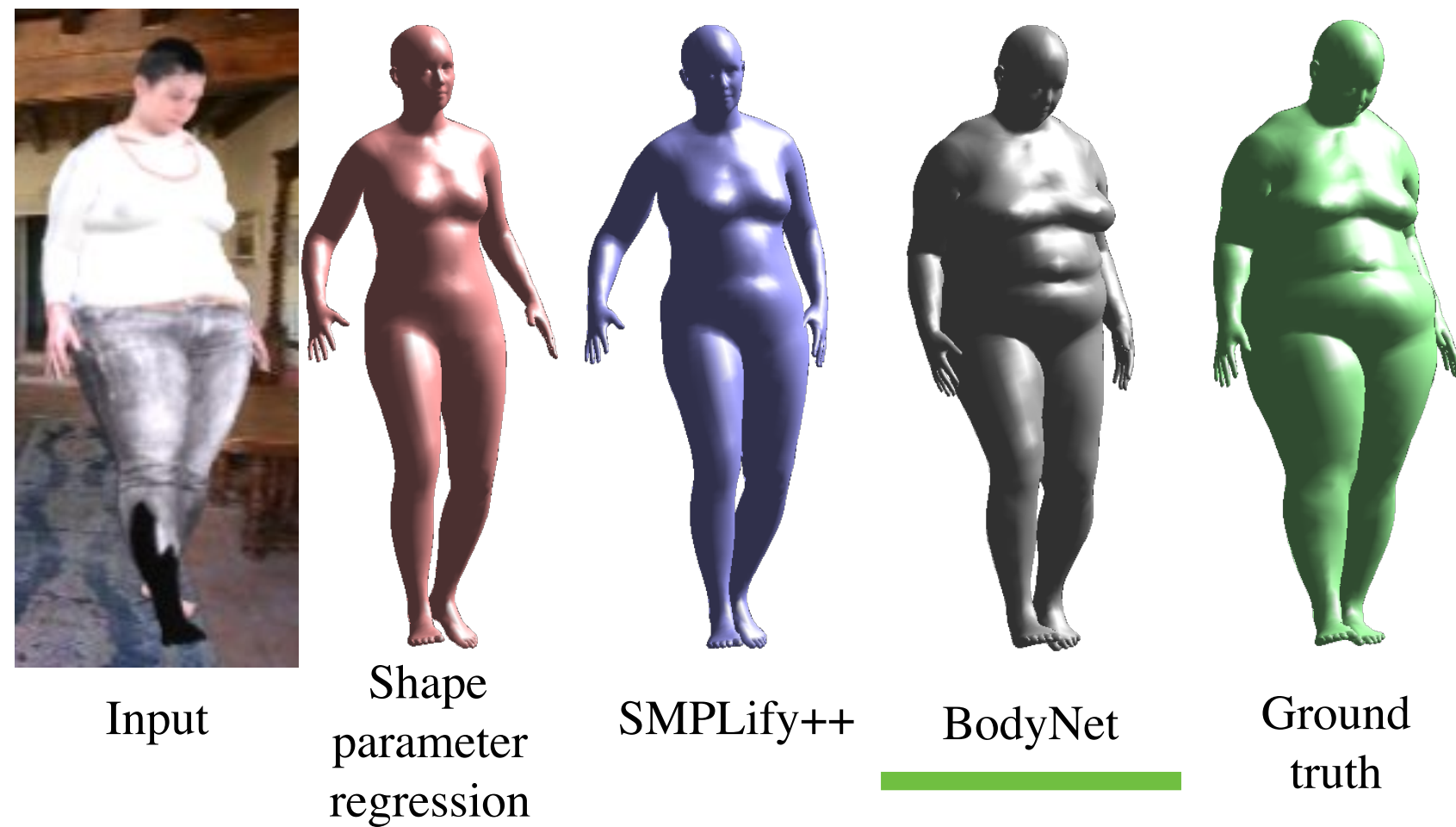
Experiments

- Effect of multi-view re-projection
- Effect of multi-task training



Experiments

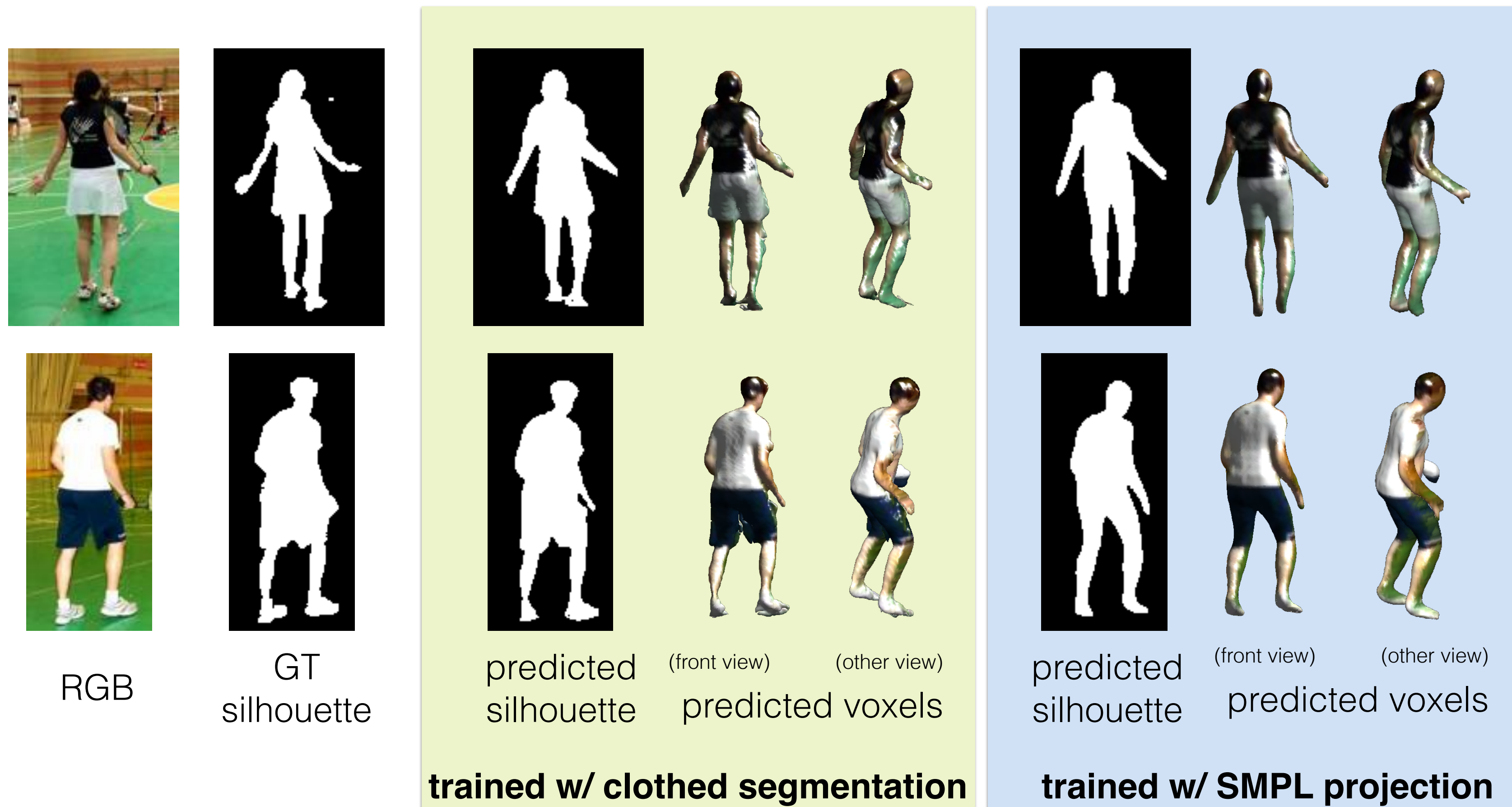
- Comparison with alternative methods



* Tung et al. Self-supervised learning of motion capture, NIPS 2017

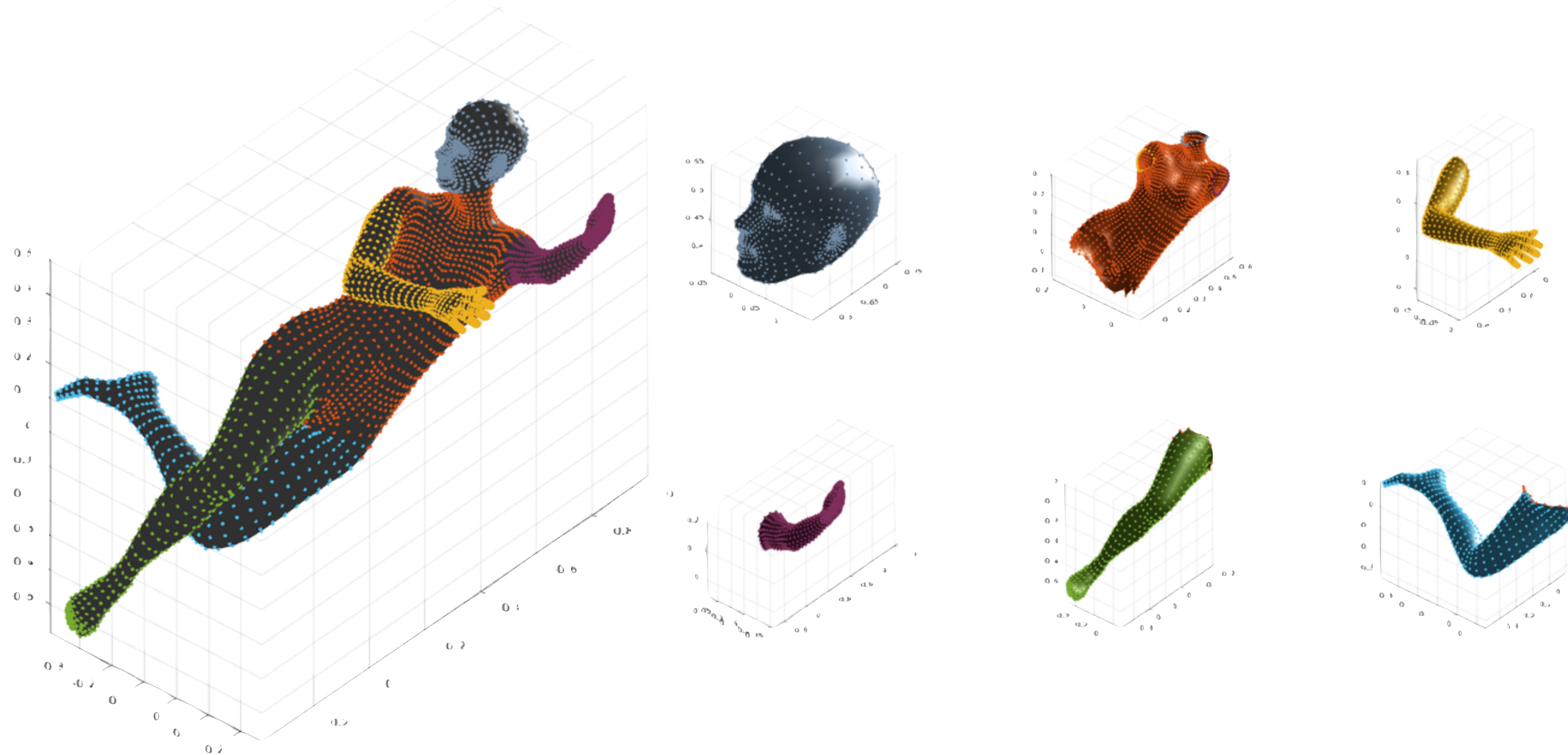
Potential to capture clothing

If the re-projection loss is supervised with 2D clothed segmentation, volumetric output captures clothing.



3D Body Part Segmentation

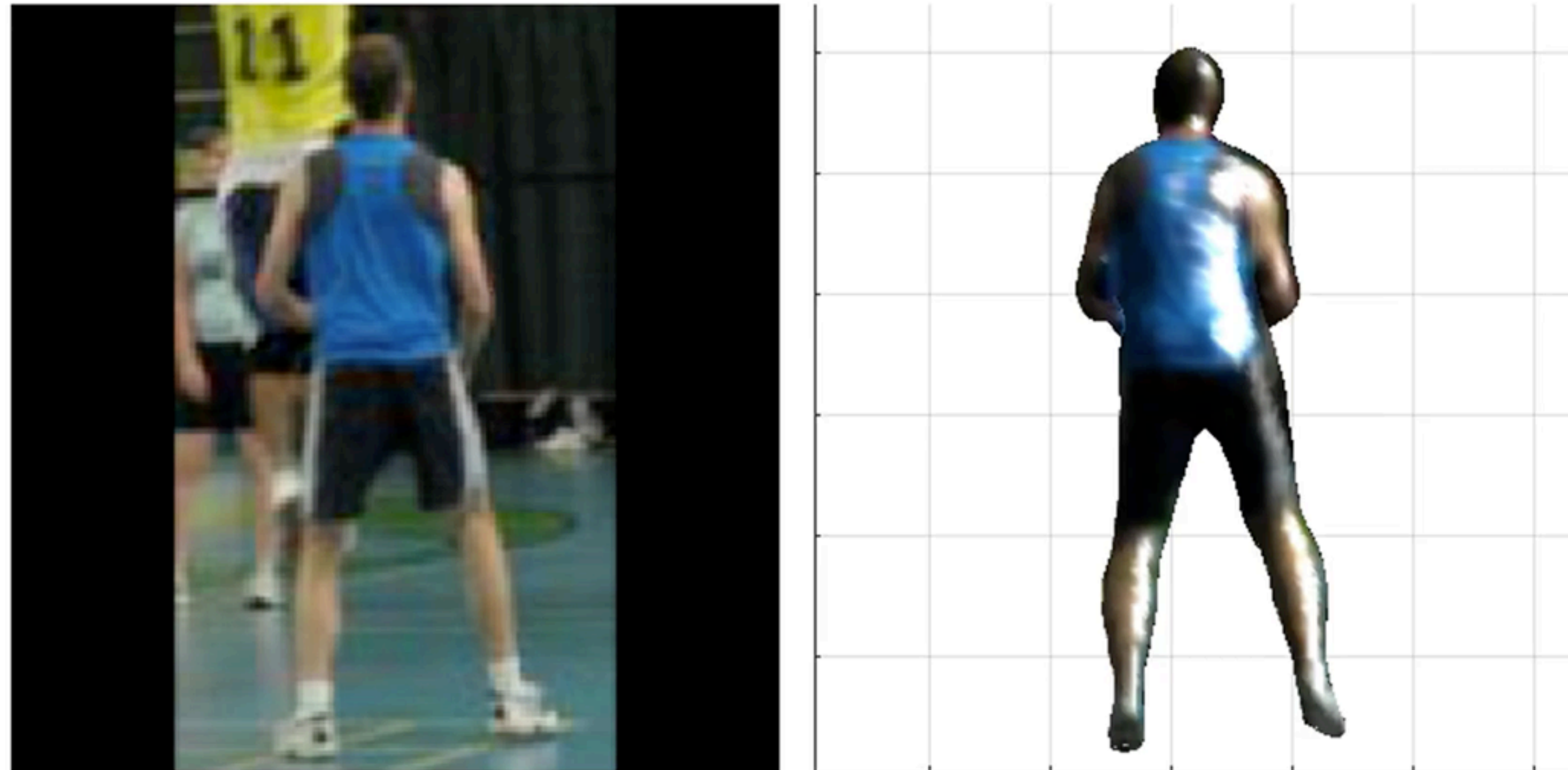
- Initialize part segmentation network with the foreground segmentation network weights by copying last layer as many times as the number of parts.



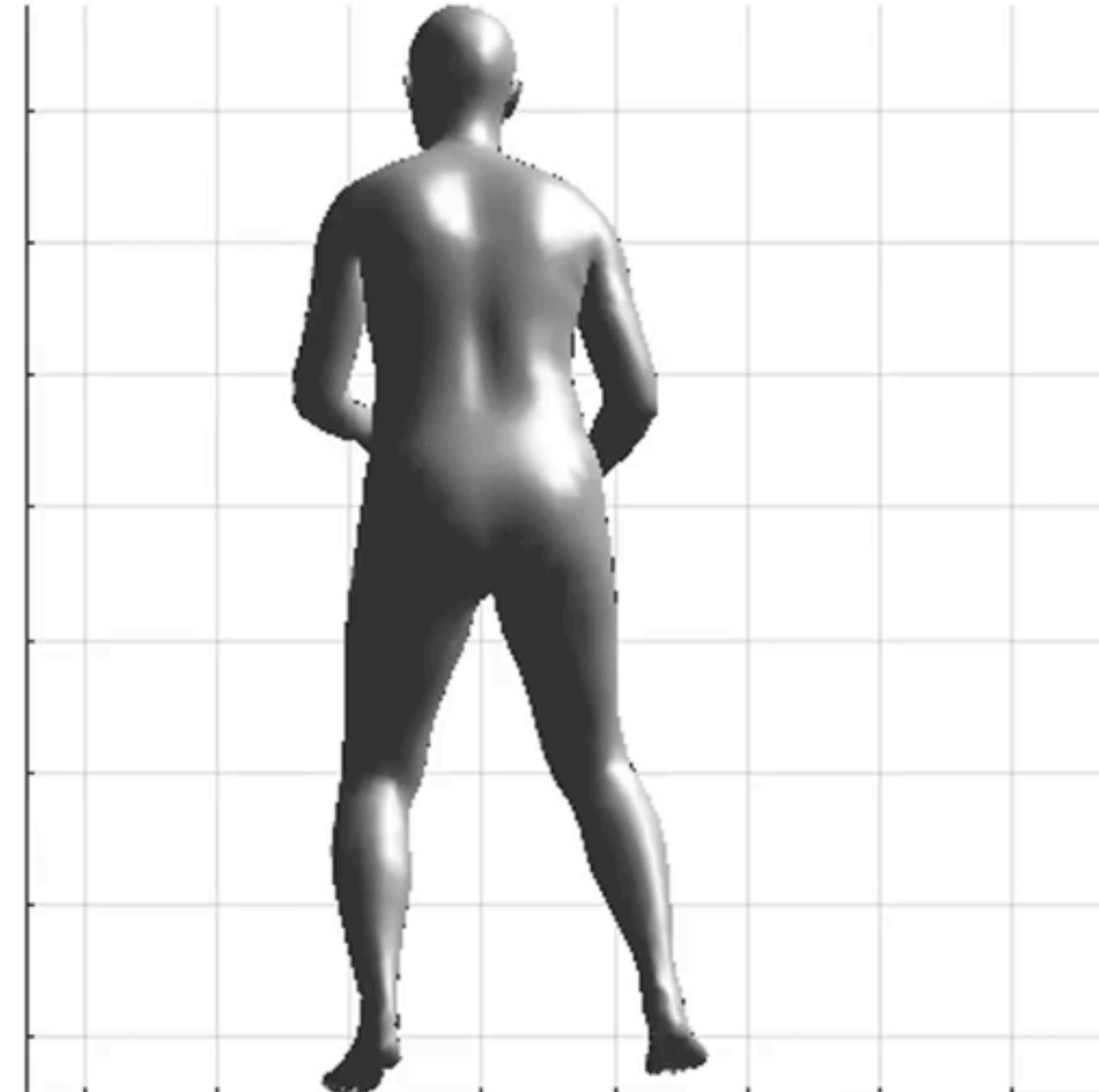
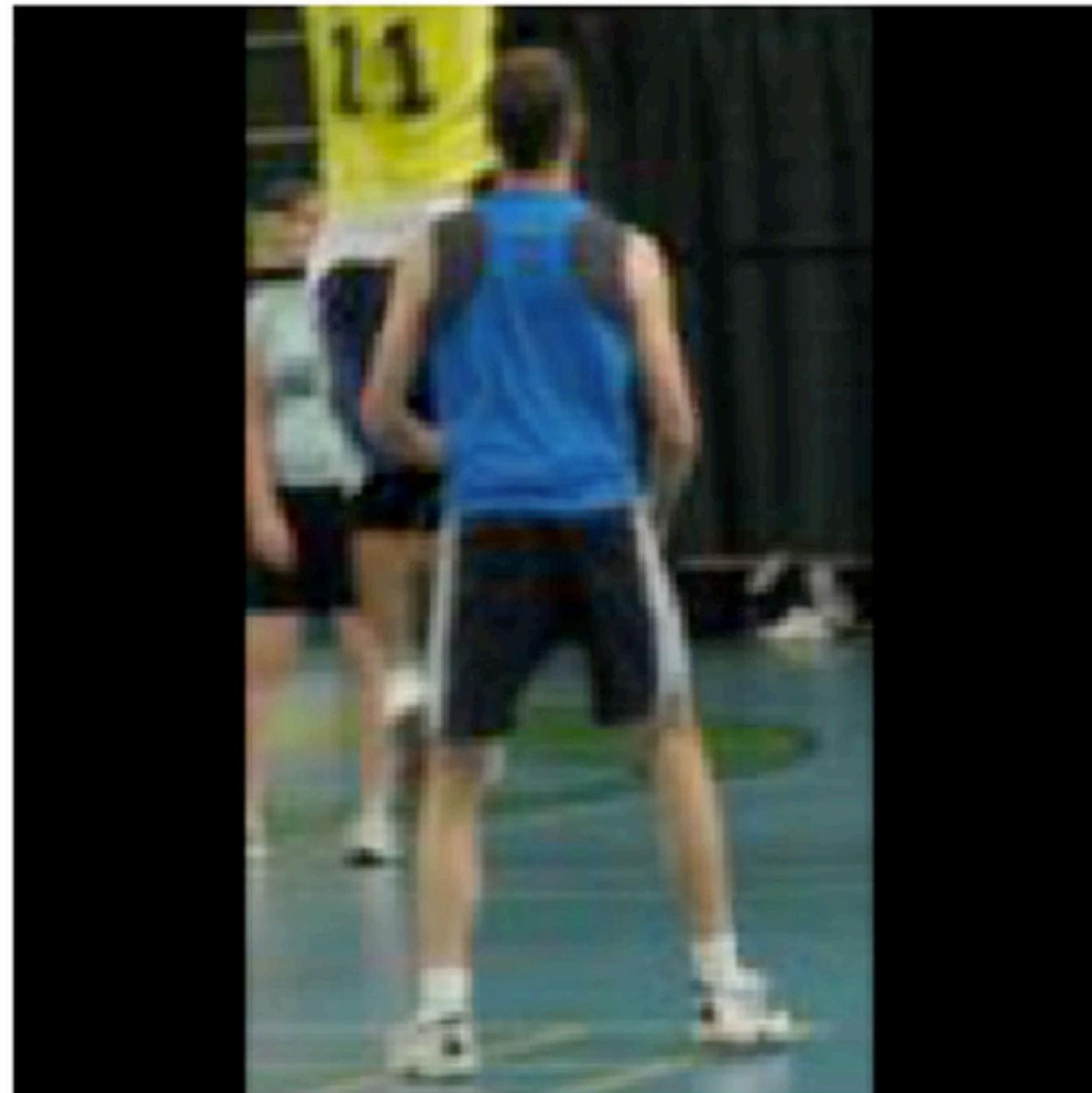
3D Body Part Segmentation



Results - Volumetric Shape



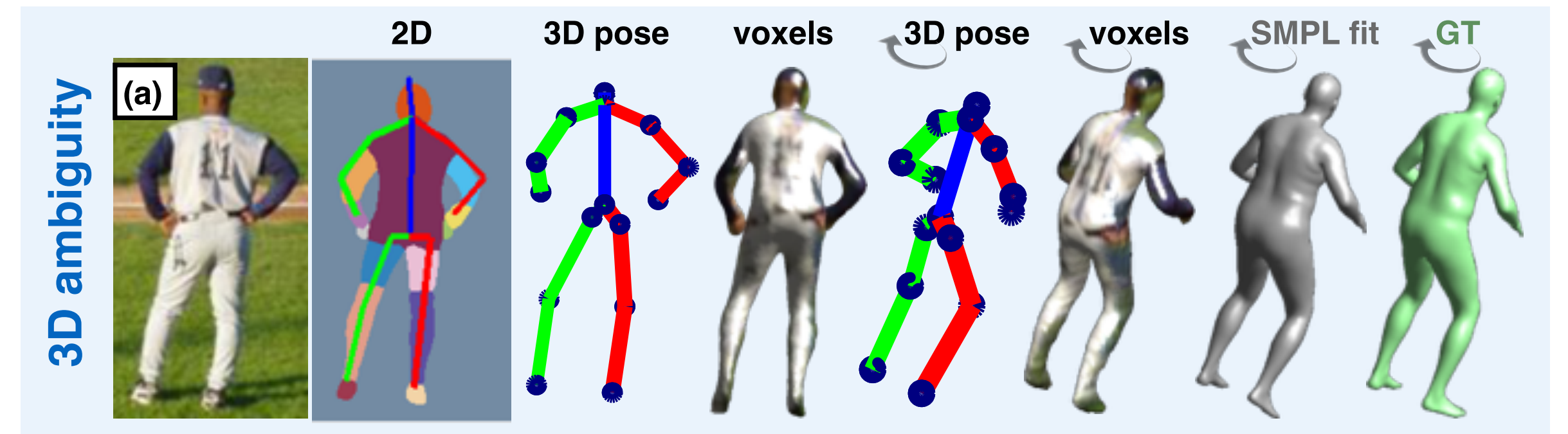
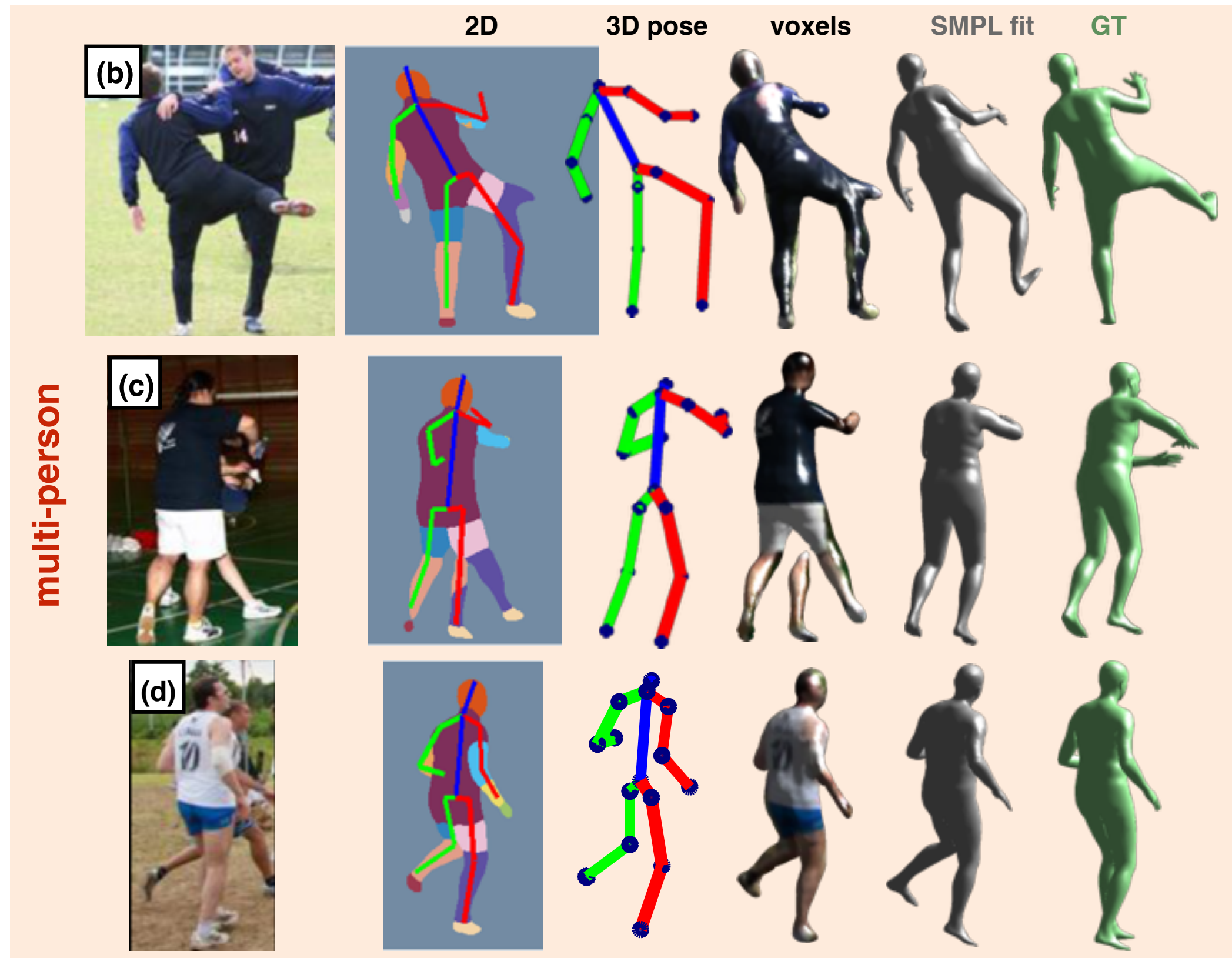
Results - SMPL fit



Results - 3D Body Parts



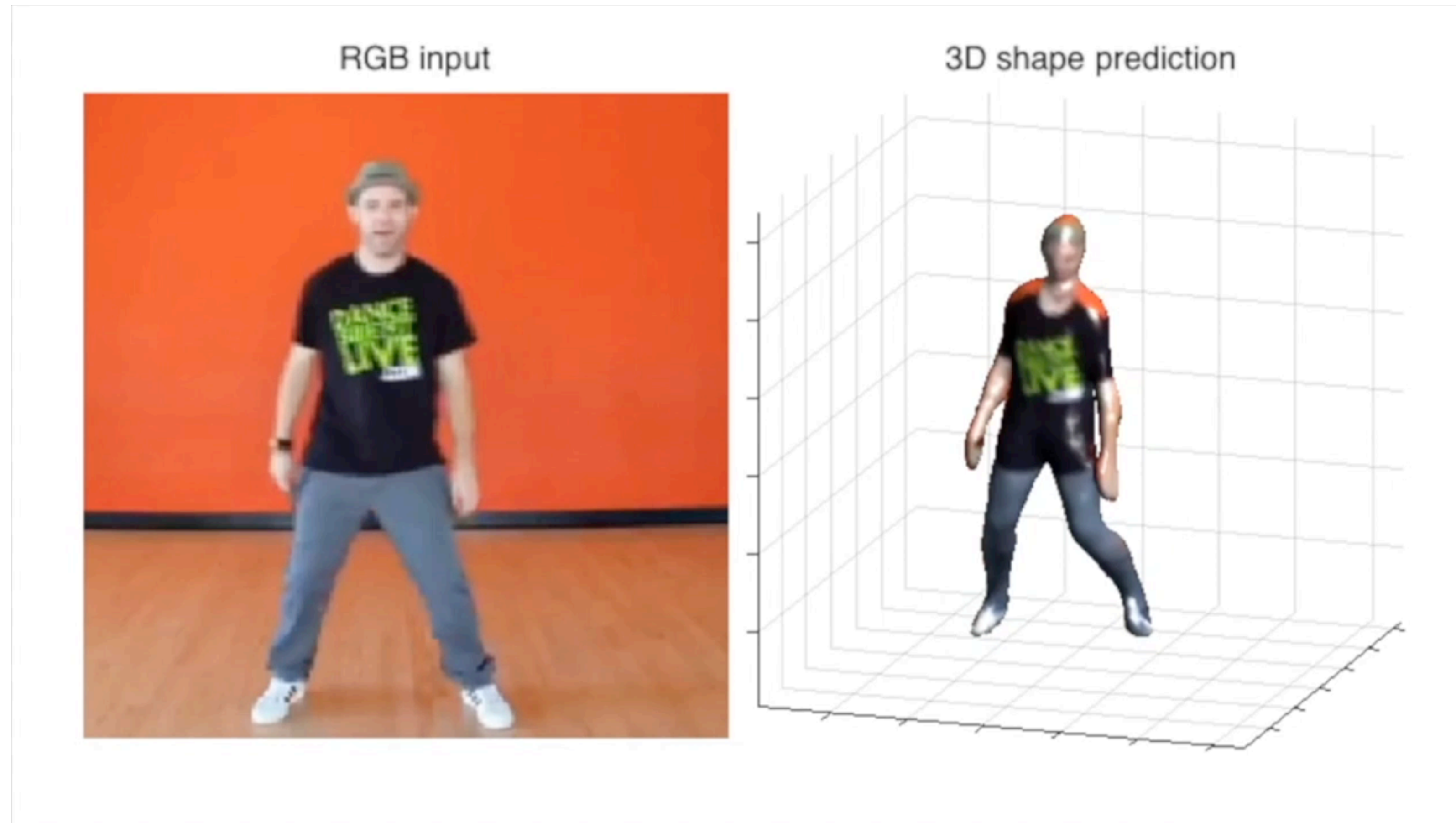
Results - Failure Cases



Conclusions

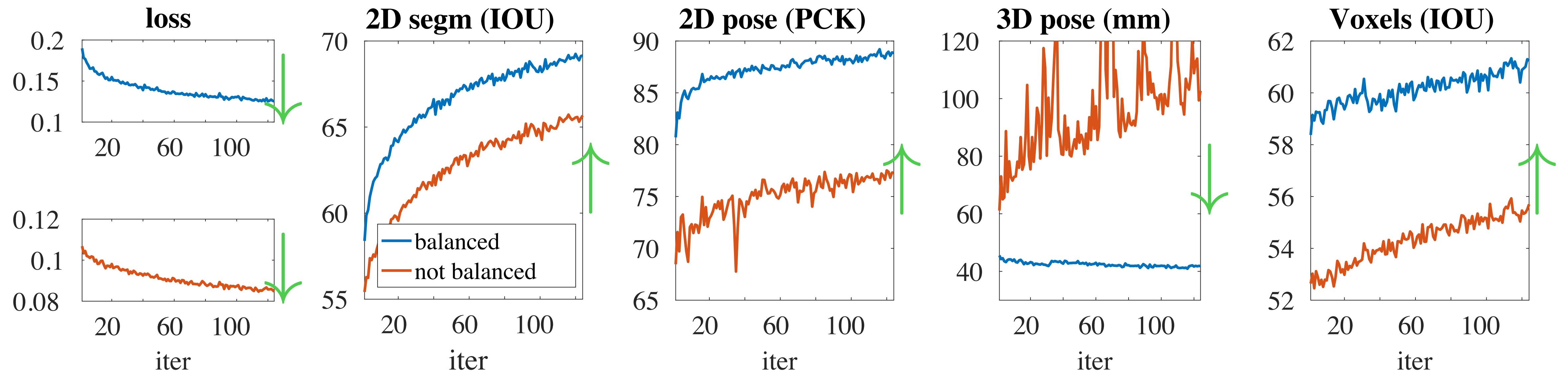
- **Volumetric** human body shape representation is a **flexible** and **effective** alternative to deformable model parameters.
- **Re-projection** loss is critical to obtain confident body surface.
- **Multi-task** training of relevant tasks such as 2D/3D pose and 2D segmentation helps 3D shape estimation.

Thanks



Code is available at:
www.di.ens.fr/willow/research/bodynet/

Balancing multi-task losses



Experiments - Unite the People

- Comparison to state-of-the-art
- Re-projection supervision

		<i>2D metrics</i>			<i>3D metrics (mm)</i>		
		Acc. (%)	IOU	F1	Landmarks	Surface	
	3D ground truth	(Lassner et al.)	92.17	-	0.88	0	0
	Decision forests	(Lassner et al.)	86.60	-	0.80	-	-
	HMR	(Kanazawa et al.)	91.30	-	0.86	-	-
⌈	SMPLify, UP-P91	(Lassner et al.)	90.99	-	0.86	-	-
	SMPLify on DeepCut	(Bogo et al.)	91.89	-	0.88	-	-
	BodyNet (<i>SMPL projections</i>)		92.75	0.73	0.84	83.3	102.5
	BodyNet (<i>manual segmentations</i>)		94.67	0.80	0.89		
<hr/>							
	3D ground truth	(Lassner et al.)	95.00	0.82	-	0	0
	Indirect learning	(Tan et al.)	95.00	0.83	-	190.0	-
⌈	Direct learning	(Tan et al.)	91.00	0.71	-	105.0	-
	BodyNet (<i>SMPL projections</i>)		92.97	0.75	0.86	69.6	80.1
	BodyNet (<i>manual segmentations</i>)		95.11	0.82	0.90		

2D Segmentation on UP



	avg macro F1
Trained with LSP SMPL projections [2]	0.5628
Trained with the manual annotations [2]	0.6046
Trained with full training (31 parts) [2]	0.6101
Trained with full training (14 parts), pre-trained on SURREAL (ours)	0.6397

occlusion



noisy labels



hair / hat



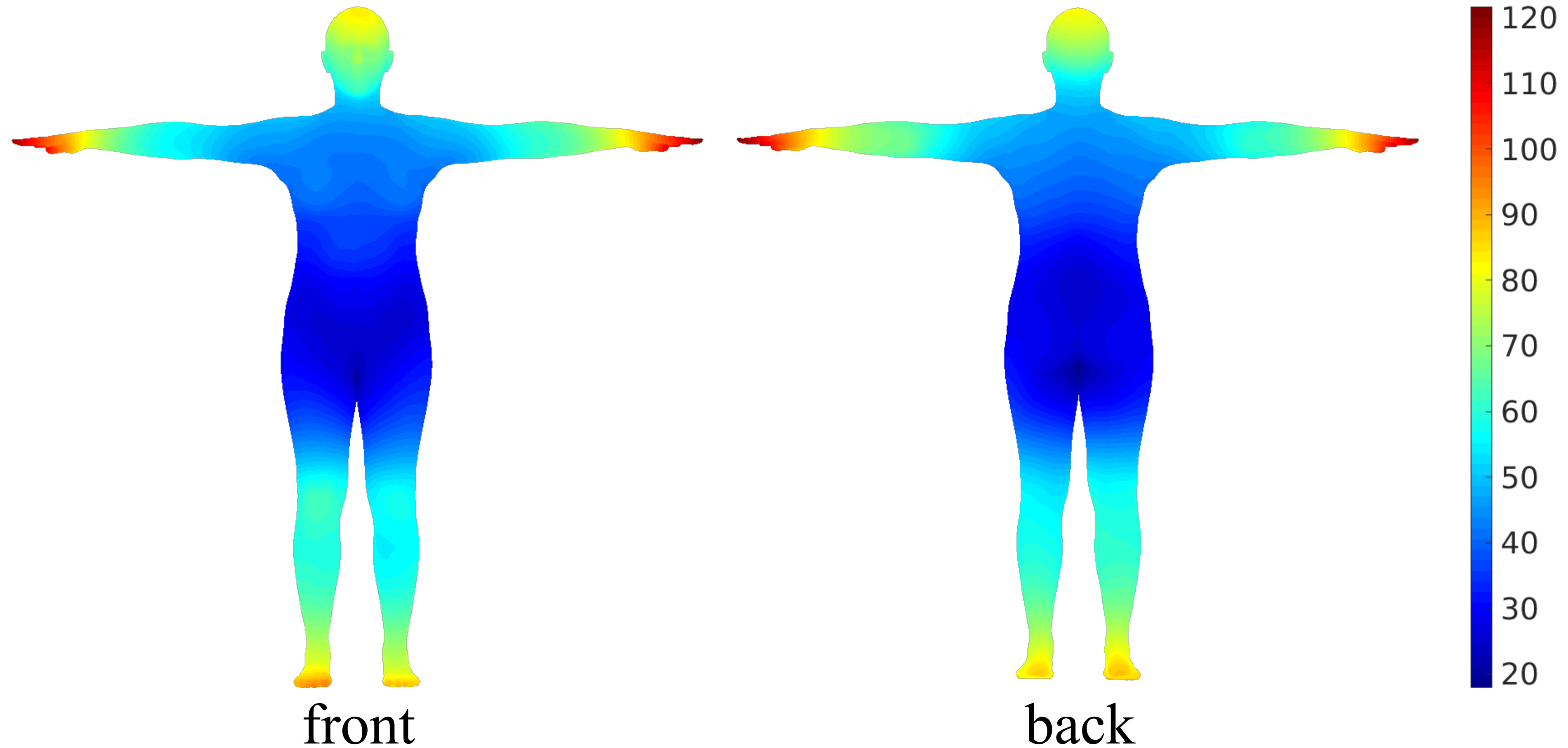
cloth deformations

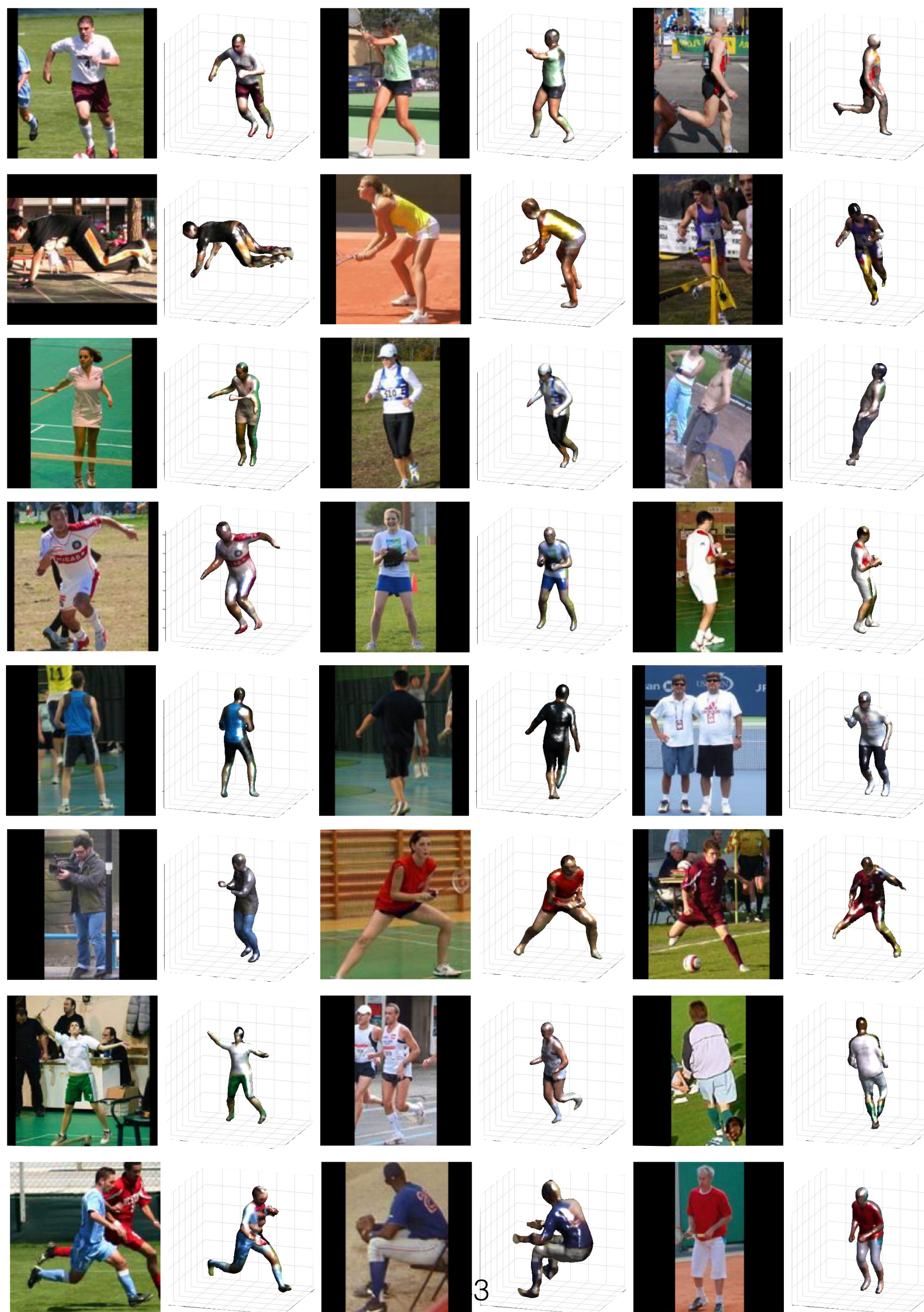


multi-label



SMPL Surface Error





Intermediate Tasks after Multi-task Fine-tuning

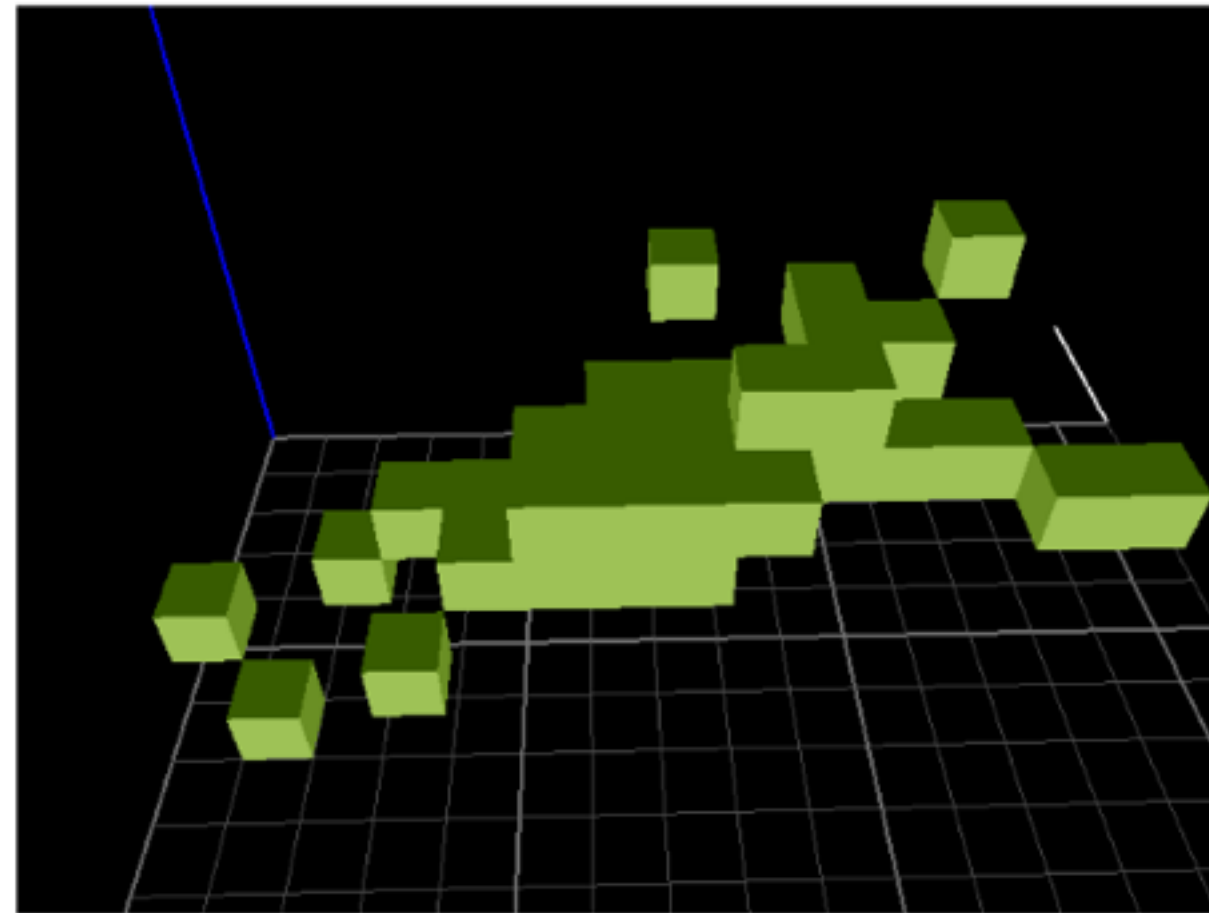
	Segmentation mean parts IOU (%)	2D pose PCKh@0.5	3D pose mean joint distance (mm)
Independent single-task training	59.2	82.7	46.1
Joint multi-task training	69.2	90.8	40.8

3D Pose Experiments

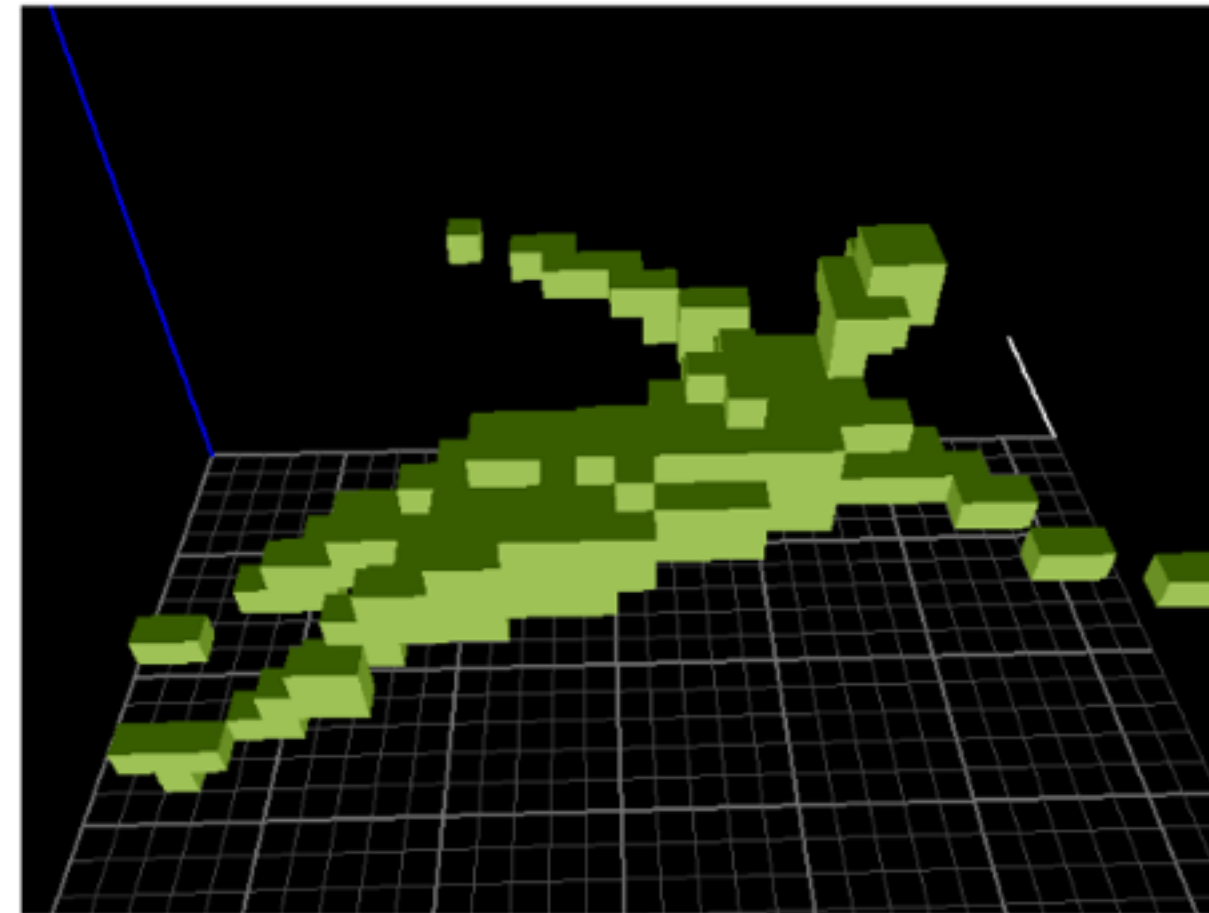
Input	SURREAL	Human3.6M
RGB	49.1	51.6
2D pose	55.9	57.0
Segm	48.1	58.9
2D pose + Segm	47.7	56.3
RGB + 2D pose + Segm	46.1	49.0
Kostrikov & Gall [9]		115.7
Iqbal <i>et al.</i> [10]		108.3
Rogez & Schmid [11]		88.1
Rogez <i>et al.</i> [8]		53.4

Voxel grid resolution

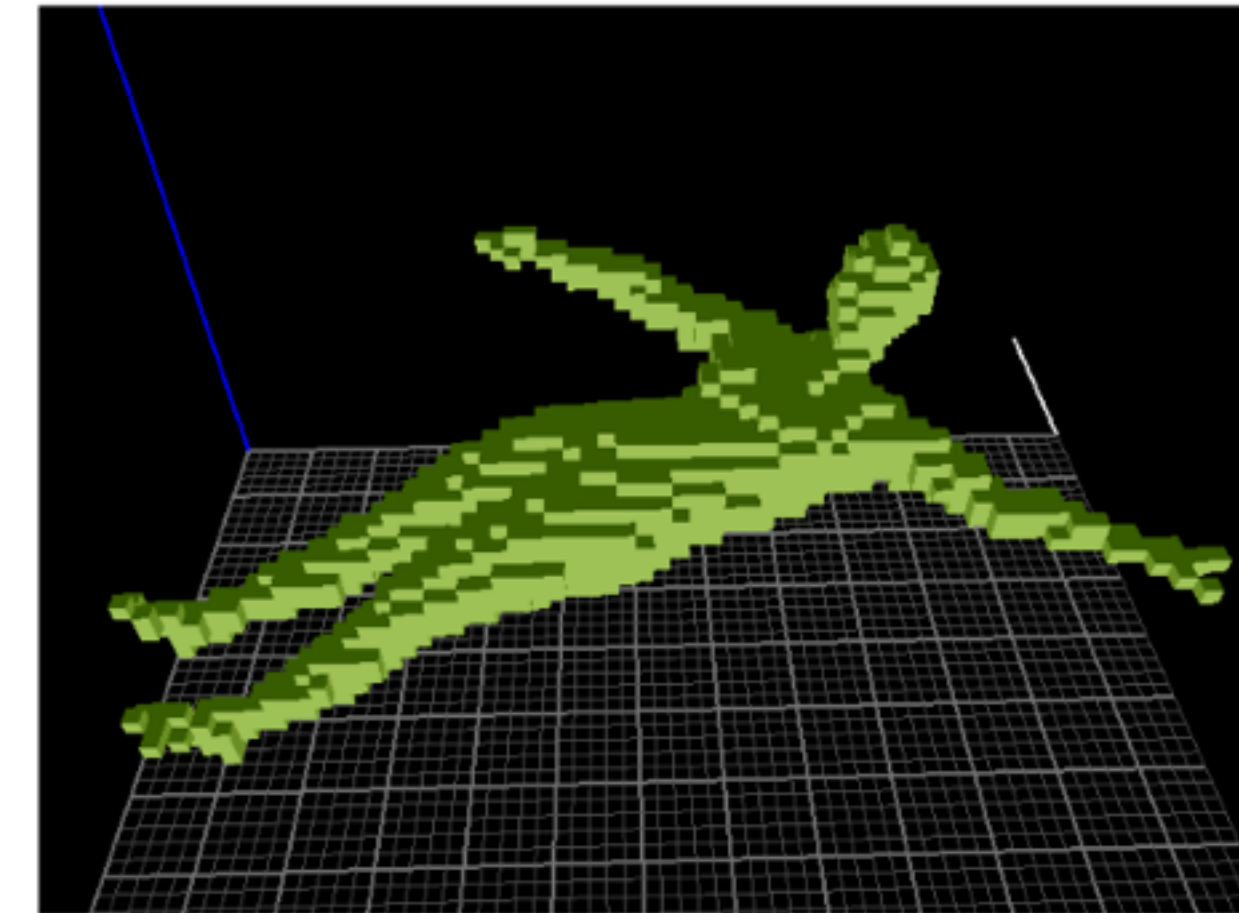
16x16x16



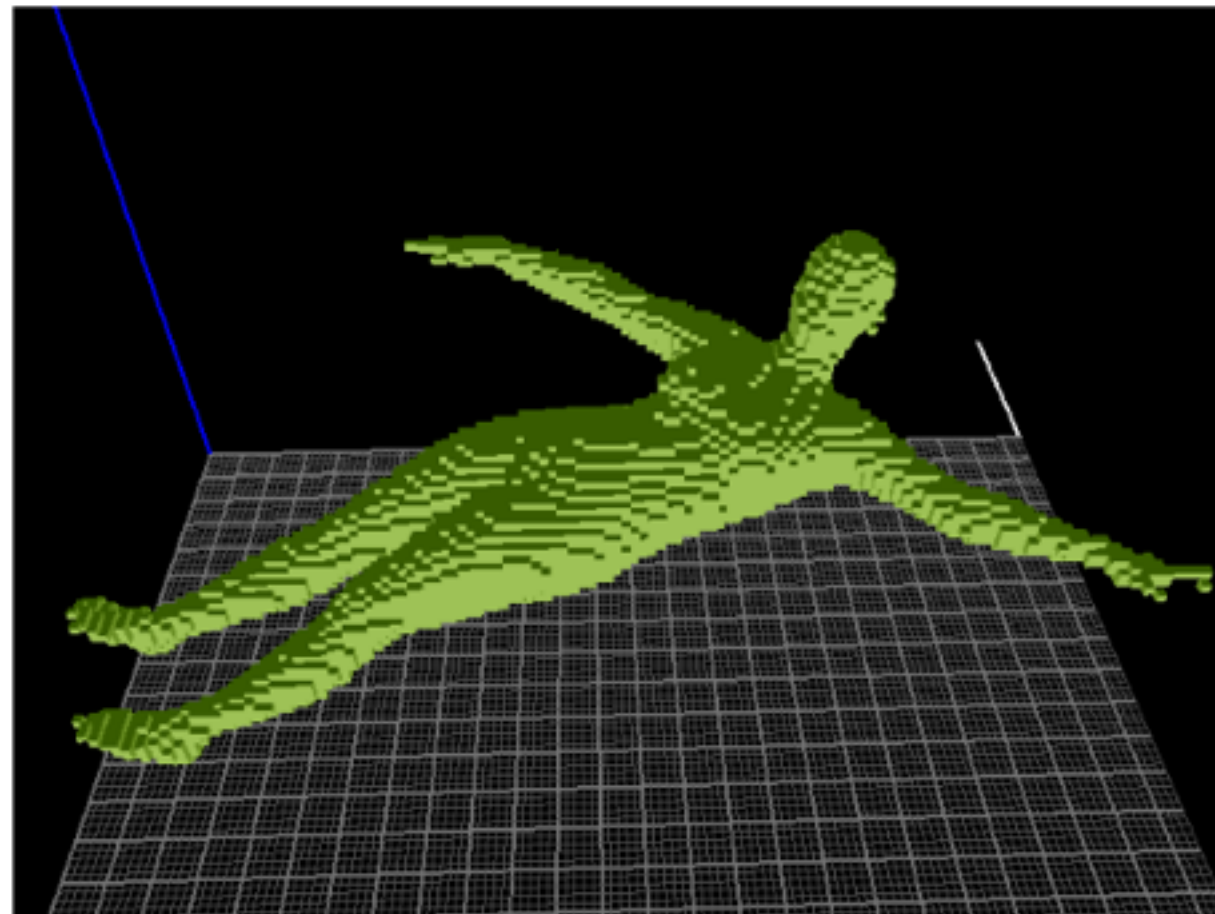
32x32x32



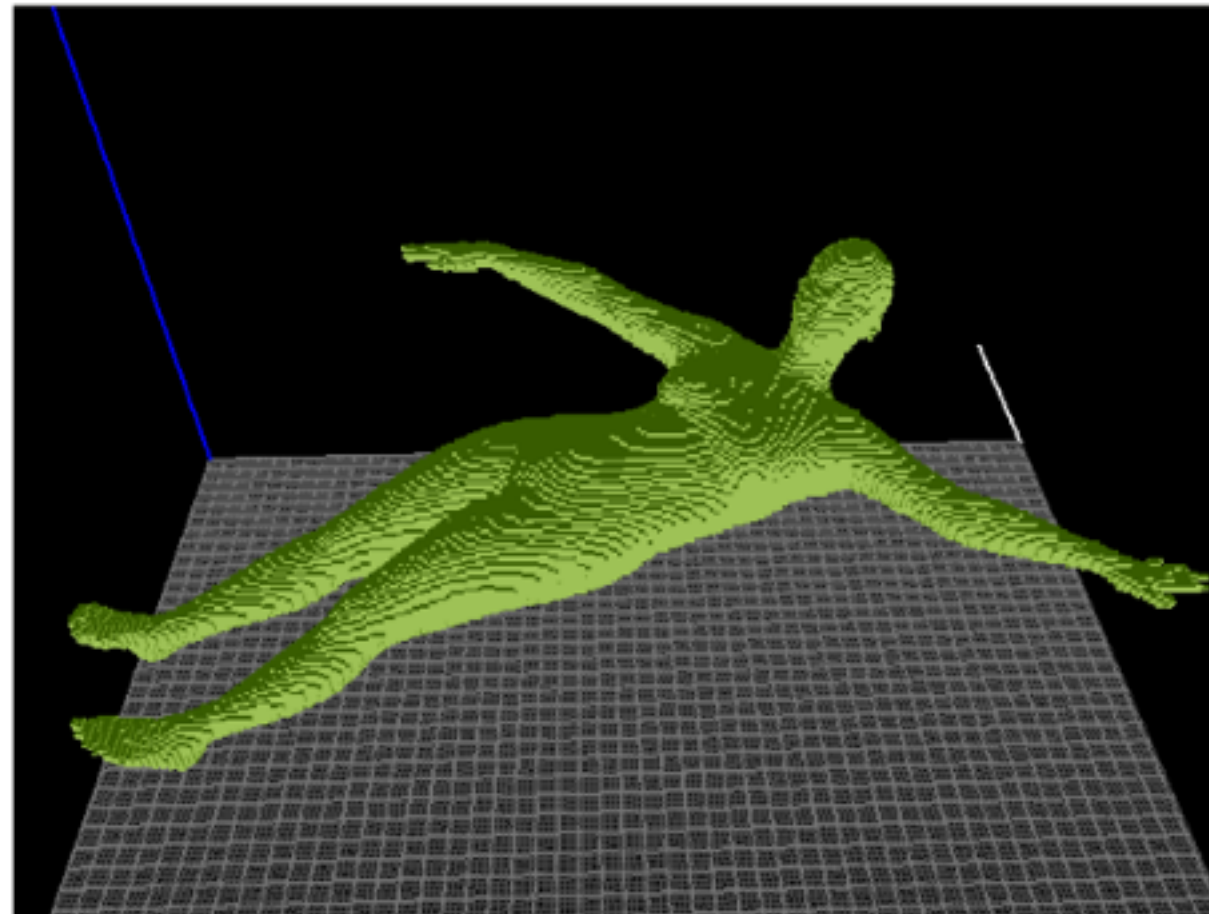
64x64x64



128x128x128



256x256x256



512x512x512

